Threat intensification reshapes trait-response relationships in birds and mammals

Sarah Bull[1], Simone P. Blomberg[3], Rikki Gumbs[2], Katrina J Davis[1], Roberto Salguero-Gómez[1]

[1]Department of Biology, University of Oxford; Oxford, United Kingdom, [2] Institute of Zoology, Zoological Society London; London, United Kingdom, [3]School of the Environment, The University of Queensland; Queensland, Australia

Email: sarah.bull@balliol.ox.ac.uk

Abstract

Predicting which species are most at risk of extinction, and by which threats, is central to effective biodiversity management (1). Trait-based frameworks, linking species traits to extinction risk, are increasingly used to predict global biodiversity trends, with applications from species-specific prioritisations (2) to estimations of global diversity loss (3). However, despite the strong spatial heterogeneity (4) and rapid acceleration of pressures globally (5), current trait-based approaches implicitly assume that trait-response relationships are stable across gradients of threat intensity. Here, we test this assumption, using a dataset of 9,262 bird and mammal responses to three key threats: habitat modification, hunting, and invasive species/disease. We show that, for all threats examined, intensification fundamentally alters how species traits mediate population responses, frequently reversing whether traits buffer or amplify declines. The shape of the interaction between threat intensity and trait effects is strongly dependent on threat type, taxa, and the degree of intensification. Our findings provide strong evidence that trait-mediated sensitivity is not intrinsic to a species, as currently assumed, but dynamic. Consequently, spatial and temporal changes in threat intensity have the potential to restructure risk across species, strongly challenging current interpretations of trait-based frameworks in predicting present and future biodiversity change. Equally, the relationship between traits and population response to intensification presents an opportunity to integrate complex, non-linear responses to intensification into biodiversity forecasts at a generalisable scale.

Main text

Biodiversity loss is pervasive (7), but rates of decline are not randomly distributed across the tree of life (3). Rather, different biological traits and exposures to threats cause species to exhibit a wide range of responses (*i.e.* changes in the rates of population growth) to environmental change (8, 9). Understanding which species are at the greatest risk of decline and how declines are likely to change

under future conditions is essential for effective conservation (1)(10). Due to resource constraints and the urgency and scale of biodiversity loss (11), generalisable predictive frameworks have become an appealing tool for large-scale biodiversity risk assessments. In this regard, comparative trait approaches have been used extensively to predict patterns of species vulnerability by exploring links between species traits and responses to environmental change (see 12 for a comprehensive review). The potential for trait-based frameworks to address major conservation challenges has been widely recognised (*e.g.* 13). Indeed, applications span ecological scales, from species prioritisation models (*e.g.* 2), to estimates of global functional diversity loss (*e.g.* 3).

Despite their widespread use, current trait-based frameworks typically implicitly assume that trait-response relationships are not affected by the intensity of the threat itself. Yet, there is growing mechanistic and empirical support for complex, non-linear population responses to threat intensification (6). At the trait-level, several mechanisms that may influence buffering/amplification dynamics as threat intensity increases. For example, biological limits on buffering capacities (14), or shifts in the demographic mechanisms by which threats operate across intensities (e.g. non-lethal to lethal effects). As a result, current trait models may mask hotspots of risk that exist only under more severe conditions or exaggerate risk for species exposed to conditions below threshold levels of threat (*e.g.* where buffering capacity is not yet surpassed). Finally, whilst current trait-based predictions may offer insight into species vulnerability under current conditions, they do not provide the much-needed understanding of how existing patterns of risk will shift in the future as pressures intensify.

The implications of non-linear response dynamics for trait-response relationships at a macroecological scale remain unknown. To address this gap in understanding, we investigate how threat intensity influences trait-based patterns of population response for three key threats: habitat modification, hunting, and invasive species/disease. Our analysis focuses on bird and mammal species, drawing on an extensive dataset of over 9,000 threat-specific measures of population response (estimated rates of decline, hereafter response severity) with associated measures of threat intensity (the proportion of a species global population exposed to threat) from the IUCN Red List (15), and key life history traits from the Amniote Life History Database (16). Exploring the interactions between population responses, threat intensity, and species traits, we show distinct patterns of buffering and sensitivity across life history trait spaces along gradients of threat intensity. We discuss the implications of non-stationary trait-response relationships for biodiversity risk

predictions across ecological scales, including both the challenges (*e.g.* limits to transferability of trait-based predictions across threat conditions) and opportunities (*e.g.* the potential for traits to estimate non-linear threat-response relationships).

Threat intensification reshapes trait responses

Species life history traits mediate population responses to threats, but patterns of buffering and sensitivity to threats are strongly affected by threat intensity. To explore how the relationship between life history traits and population responses to threats varies with threat intensity, we modelled the effects of species positions in the life history trait space on population responses under increasing threat intensity. We defined the life history trait spaces for birds and mammals through a principal component analysis (PCA) on nine key life history traits in birds, and eight in mammals. For birds (Figure 1A), variation in life history strategies generally lies along a diagonal reflecting the slow-fast continuum (17, 18), with reproductive outputs trading off against developmental pace and size-associated traits on both the first and second axes. For mammals (Figure 1B), the first axis (PC1) reflects the fast-slow continuum (17, 18), whilst the second axis (PC2) captures an additional trade-off between body size and litter size against developmental pace. The majority of variation in life history strategies is explained by these two axes in both birds and mammals (Figure 1, 80.3% and 82.0% of total variation explained in bird and mammal trait spaces, respectively; for more details, see Supplementary Materials: Bird and mammal life history trait spaces).

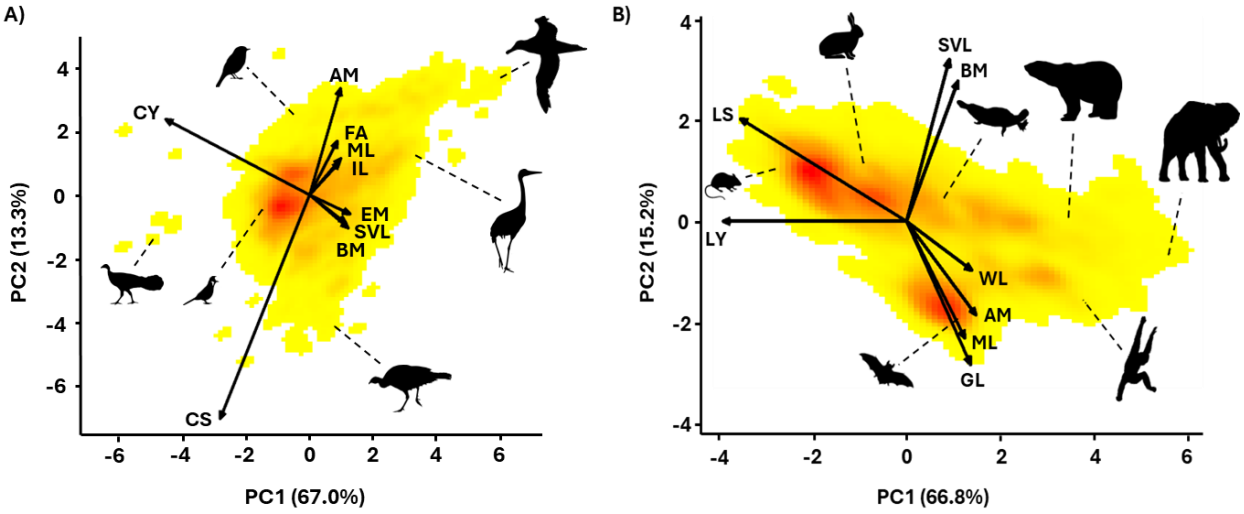

Figure 1: Most variation in life history strategies across birds and mammals can be described by two key axes of trait variation. Trait density profiles describing the occupation of (**A**) the examined 8,497 bird species and (**B**) 3,364 mammal species within their life history trait spaces, defined by the first two principal component axes of a principal component analysis (PCA). The proportion of trait variation explained is shown for each axis. Red colour represents regions of higher species density, while yellow represents lower density. Traits for birds include: maximum longevity (ML; years), age of maturity (AM; days), clutch size (CS), clutches per year (CY), incubation length (IL; days), fledgling age (FA; days), egg mass (EM; grams), adult body mass (BM; grams), and adult snout-vent length (SVL; cm). Traits for mammals include: maximum longevity (ML; years), age of maturity (AM; days) litter size (LS), litters per year (LY), gestation length (GL; days), weaning length (WL; days), adult body mass (BM; g), and adult snout-vent length (SVL; cm). Arrows represent the direction and weighting of each life history trait in the PCA space (for full loadings see supplementary tables 1 & 2). For birds (A) silhouettes correspond to (starting from top right and moving clockwise): Tristan albatross (*Diomedea dabbenena*), Red-Crowned Crane (*Grus Japonensis*), Wild turkey (*Meleagris gallopavo*), White-eared bulbul (*Pycnonotus leucotis*), Australian brushturkey (*Alectura lathami*), and Lemon-bellied flyrobin (*Microeca flavigaster*). For mammals (B) silhouettes correspond to (starting from top right and moving clockwise): Platypus (*Ornithorhynchus anatinus*), Polar bear (*Ursus maritimus*), African bush elephant (*Loxodonta africana*), Yellow-cheeked gibbon (*Nomascus gabriellae*), Bechstein's bat (*Myotis bechsteinii*), House mouse (*Mus musculus*), and Snowshoe hare (*Lepus americanus*). All silhouettes were downloaded from PhyloPic (www.phylopic.org).

Here, we define threat intensity as the proportion of a species global population exposed to the threat (low intensity: <50% population exposed, moderate intensity: >50% but <90% population exposed, and high intensity: >90% population exposed, following IUCN population scope categories, 15). We examined how patterns of response across bird and mammal life history trait spaces vary at each level of intensity for three key threats: habitat modification, hunting, and invasive species and disease (birds only due to mammal data limitations). Our results reveal extensive variation in the strength, and indeed existence, of trait effects along gradients of intensity for all threats (Figures 2 & 3). Whether the magnitude of trait effects increases or decreases with intensification is highly specific to threat type, taxa, and position in the trait space.

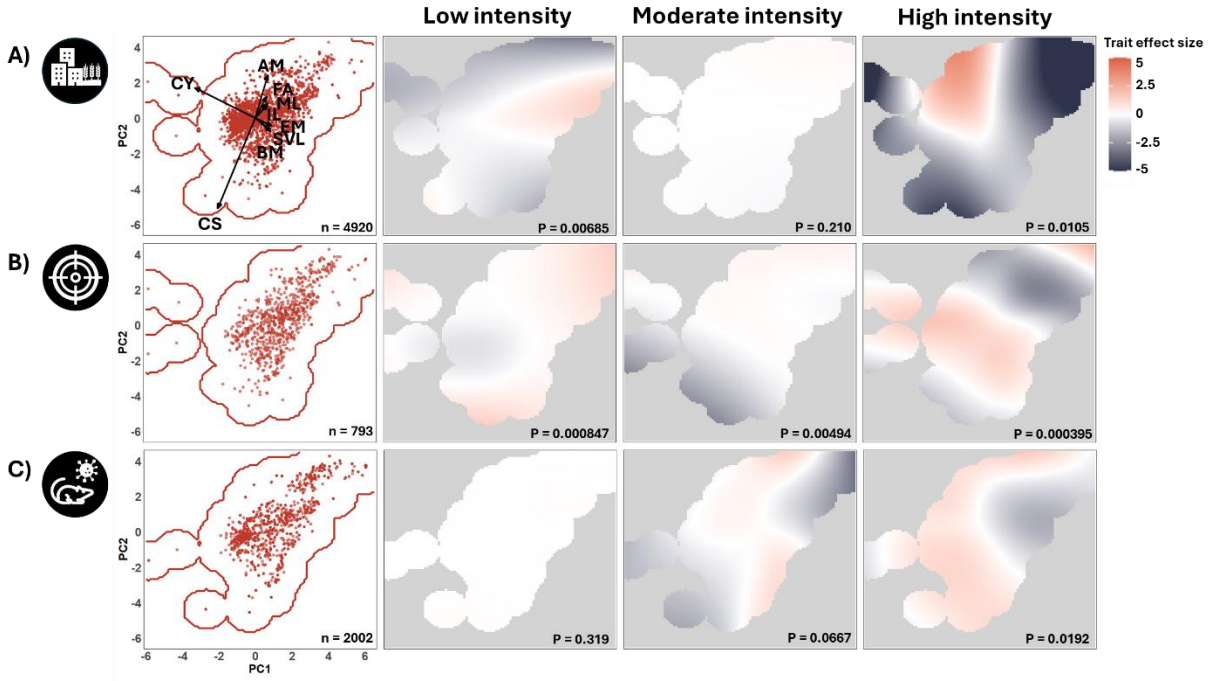

Figure 2: Trait-mediated patterns of threat response are strongly dependent on threat intensity in birds. Model estimates for the effect sizes of life history traits on the severity of bird population responses to (**A**) habitat modification, (**B**) hunting, and (**C**) invasive species/disease, visualised across the life history trait space at low, moderate, and high intensity. Predictions were obtained from phylogenetically corrected GAMs. The left column illustrates the distribution of data used in models across the bird life history trait space (red points), corresponding confidence bounds of the model in the trait space (red contour), and the loadings of the trait space. Loading acronyms correspond to the following traits: age at maturity (AM; days), fledgling age (FA; days), maximum longevity (ML; years), incubation length (IL; days), egg mass (EM; grams), adult snout-vent length (SVL; cm), adult body mass (BM; grams), clutch size (CS), clutches per year (CY). Within effect size plots, dark red represents positive effects of life history traits on the severity of population response (greater-than-average response severity, *i.e.* amplification). Dark blue represents negative effects of life history traits on the severity of population response (lower-than-average response severity, *i.e.* buffering). White areas represent regions of low trait effects, where population response is close to the average response attributable to intensity only. We do not extrapolate responses for regions of the trait space that fall outside of the model confidence intervals (grey areas, see also red contour lines in left panel). P-values for the significance of trait effects (derived from the GAMs, approximate X^2 tests) are shown for each level of intensity in the bottom right of effect plots. The number of species responses used in each model is shown in the bottom right of the left column.

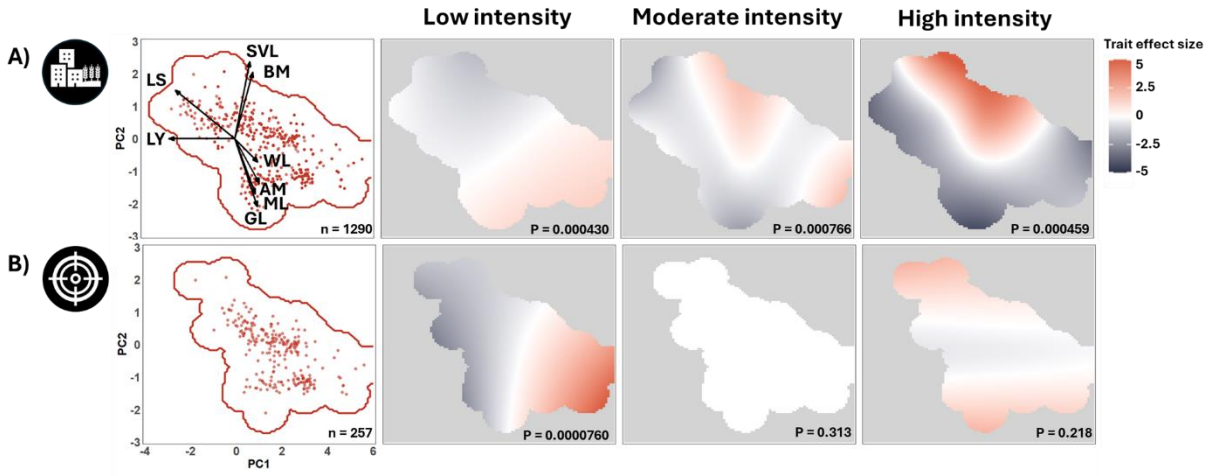

Figure 3: Trait-mediated patterns of threat response are strongly dependent on threat intensity in mammals. Model estimates for the effect sizes of life history traits on the severity of mammal population responses to (**A**) habitat modification, and (**B**) hunting, visualised across the life history trait space at low, moderate, and high intensity. Predictions were obtained from phylogenetically corrected GAMs. The left column illustrates the distribution of data used in models across the trait space (red points), corresponding confidence bounds of the model in the trait space (red contour), and the loadings of the trait space. Loading acronyms correspond to the following traits: adult snout-vent length (SVL; cm), adult body mass (BM; g), weaning length (WL; days), age of maturity (AM; days), gestation length (GL; days), maximum longevity (ML; years), litters per year (LY), litter size (LS). Within effect size plots, dark red represents positive effects of life history traits on the severity of population response (greater-than-average response severity, *i.e.* amplification). Dark blue represents negative effects of life history traits on the severity of population response (lower-than-average response severity, *i.e.* buffering). White areas represent regions of low trait effects, where population response is close to the average response attributable to intensity only. We do not extrapolate responses for regions of the trait space that fall outside of the model confidence intervals (grey areas, see also red contour lines in left panel). P-values for the significance of trait effects (derived from the GAMs, approximate X^2 tests) are shown for each level of intensity in the bottom right of effect plots. The number of species responses used in each model is shown in the bottom right of the left column.

The capacity of bird and mammal life history strategies to buffer against the impacts of threats is strongly dependent on the level of threat intensity. Within the same threat, species that exhibit buffered responses (*i.e.* lower than average population response severity, negative effect size) at low intensity are often equally sensitivity relative to other species under high intensity. For instance, at low intensity, the response of mammals to hunting is strongly mediated by species positions across the fast-slow continuum (17, 18) (Figure 3B, $p = 0.000076$). Species with faster strategies (low scores along PC1, *e.g.* mice and rats), are buffered against declines, whilst species with slow strategies (high scores along PC1, *e.g.* elephants) are highly sensitive (Figure 3B). The heightened response of slow-living mammal species to hunting aligns with numerous previous findings (9, 19). This effect is likely related to the high demographic sensitivity of such life history strategies to reductions in adult survival, *i.e.* population growth for slow-lived species is strongly mediated by the survival of adults (20). By moderate hunting intensity, however, we find no difference in response severities across the trait-space (Figure 3B, $p = 0.313$), and trait effects remain non-significant under high intensity (Figure 3B, $p = 0.218$). The breakdown of buffering patterns and the homogenisation of responses with increasing threat intensity suggests the existence of buffering thresholds (14), beyond which species traits no longer have the capacity to mitigate responses. For instance, adult mortality may be buffered by high reproductive rates and fast growth (19). Indeed, where density-dependent effects are acting on population a reduction in adult survival can even promote greater rates of population growth by relaxing competition (21). As threats intensify, however, this mechanism may break down as biological limits for individual reproduction are approached, and there are no longer enough reproducing adults to replenish losses. Under such dynamics, once thresholds have been exceeded, we would expect all species, regardless of reproductive capacity, to experience increasingly severe declines, reducing variability in responses across the trait space. Species-specific limits in buffering mechanisms have been identified across the literature, including in the context of invasive species (22) and climate effects, both for plants (23) and for reptiles (24). Our findings support this evidence base, emphasising that it is likely to be a widespread pattern across bird and mammal responses to threats. Critically, the location of buffering thresholds appears to depend on a species' position across the life history trait space and the threat type.

Threat intensification is not exclusively associated with the homogenisation of population responses across the trait space (i.e. a reduction in trait effects). Rather, we find that, under many threat scenarios, the magnitude of trait effects increases with intensity. This trend is observed across bird responses (Figure 2) and is particularly strong in the case of invasive species and disease (Figure

2C). There is no statistically significant variation in the response of bird populations to invasive species and disease across the life history trait space at low (Figure 2C, p = 0.319) or moderate intensity (Figure 2C, p = 0.0667). Significant trait effects only emerge in population responses to high threat intensity (Figure 2C, p = 0.0192). Under high intensity, we observe substantial buffering in species with slower paces of life and large body sizes (high scores along PC1 and PC2, *e.g.* cranes and large raptors). Conversely, species with faster paces of life and smaller body sizes (low scores along PC1 and PC2, *e.g.* small passerines) exhibit sensitivity under high intensity. A similar trend is observed in bird responses to habitat modification (Figure 2A) and, to a lesser extent, hunting (Figure 2B), for which the greatest magnitudes of trait effects are observed under high intensity. The emergence of stronger trait patterns at higher intensities does not preclude the existence of buffering thresholds. Rather, it may suggest that thresholds for most species exist at higher levels of intensity. For instance, most species across a taxon may exhibit some capacity to buffer against the impacts of a threat at low intensity (*e.g.* dispersal mechanisms in birds), resulting in lower differences in response across the trait space. In a review of the position of response thresholds to landscape change in bird species, (25) found that threshold responses (*i.e.* greater sensitivity to additional land-use change) emerged on average at 33.6% mean habitat cover in tropical latitudes and 27.9% in temperate latitudes. It is possible that when exposure to a threat lies above response thresholds, trait-based differences in susceptibility across populations are diluted or even masked.

Finally, under some threats, intensification restructures the direction of trait effects. Across models, we identify regions of the trait space where species are buffered under low threat intensity but become sensitive under high threat intensity. Equally, regions where species are sensitive under low threat intensity can become relatively buffered under high threat intensity. For example, in mammals, species with slower paces of life (high scores along PC1) exhibit sensitivity to low intensity habitat modification (Figure 3A). Under moderate threat intensity, the hotspot of sensitivity shifts towards species with moderate paces of life, although only for those with relatively large body sizes (moderate scores along PC1, high scores along PC2). The trend continues under high intensity, with sensitivity shifting towards species with faster paces of life and relatively large body sizes (low scores along PC1, high scores along PC2). As a result, species occupying the upper left region of the trait space, with faster paces of life but relatively large body sizes (*e.g.* rabbits and hares), revert from being the most buffered species at low intensity to the most sensitive species at high intensity. Conversely, species occupying the lower middle region of the trait space, with moderate to slow paces of life and relatively small body sizes (*e.g.* bats), exhibit high sensitivity to low intensity habitat

modification, yet become the most buffered species under high intensity habitat modification. Similar reversals in the direction of trait effects are also observed in bird responses to habitat modification (Figure 2A). Species with slower paces of life and larger body sizes (high scores along PC1 and moderate-high scores PC2, *e.g.* cranes) exhibit the highest sensitivity under low levels of habitat modification yet become the most buffered under high intensity.

Shifts in the direction of trait effects as threat intensity increases may indicate differences in the acceleration of risk once thresholds of buffering capacity have been surpassed. Equally, directional shifts may suggest fundamental changes in how threats operate on species as the threats intensify. Different threat types can disadvantage distinct life history strategies as a result of their impacts on different demographic processes. For example, hunting causes direct mortality, disproportionately impacting slow-living species (9), whereas land-use change may have more indirect effects, such as reduced reproductive capacity, with stronger consequences for fast-living species (9). Similarly, threat intensification may alter the demographic mechanisms through which threats operate. For example, low-intensity habitat modification might primarily reduce resource quality or availability, lowering reproduction or juvenile survival, whereas higher threat intensities might be associated with direct adult mortality, reshaping demographic impacts and relative patterns of trait sensitivity. Threat intensification could also modify trait responses if novel conditions create compensatory opportunities. For example, long-term monitoring of yellow-bellied toads (*Bombina variegata*) across anthropogenic habitats showed reduced survival can be offset by increased recruitment facilitated by human-created breeding sites (*e.g.*, livestock troughs or vehicle ruts in logged forests; 26). If such compensatory responses scale positively with threat intensity, intensification could substantially alter net demographic effects, reshaping relative trait-based responses. Compensatory mechanisms may be particularly relevant where initial sensitivity stabilises to relative buffering under higher intensities. Further analyses of the demographic consequences of threats at distinct levels of intensity will be critical to clarify the mechanisms driving changes in trait sensitivity.

Implications for conservation policy

Species traits, particularly those associated with their life histories (*e.g.* generation time, longevity, age at maturity), have repeatedly proven to predict species responses to threats (12). These efforts have turned trait-based frameworks into a valuable tool in conservation management (27, 13). Given the spatial variability of threat conditions (4) and the acceleration of environmental change (5), it is

critical to understand whether trait-based patterns of sensitivity to threats are constant across gradients of threat intensity. Here, we show that threat intensity does not additively affect how populations respond to threats but frequently transforms the magnitude and direction of trait-response relationships. Further, the shape of interaction between threat intensity and trait effects is highly variable across threat type, taxa, and the scale of threat intensification. Thus, we argue that trait-mediated sensitivity is not intrinsic to a species but depends on the environmental regime to which a species is exposed. This condition implies considerable limits on the transferability of trait-informed predictions across spatial and temporal gradients of threat intensity.

We identify several implications of our findings for conservation decisions across ecological scales. First, trait-based approaches are often used to estimate relative risks of extinction across species and prioritise resources, including for (re)assessments, monitoring, and active management (e.g. 27, 28). By assuming trait-mediated sensitivity remains stable across variable threat conditions, these models risk under- and over-estimating the relative sensitivity of species under current and future conditions. For instance, we find evidence that buffering mechanisms against a threat may break down beyond given thresholds of intensity (*e.g.*, mammal responses to hunting under moderate and high intensity). In such cases, species that are assumed to be intrinsically less sensitive to a threat may in fact be at equal -if not greater- risk than other species when exposed to conditions more intense than those under which models were inferred. Failing to account for these dynamics could lead to underestimation of current species vulnerability and to sudden, unexpected declines under future intensification of threats. The existence of threshold-type patterns in trait-mediated sensitivity may also influence cost-benefit relationships in species management. For example, given a set of species exposed to the same intensity of a given threat, current trait models would typically prioritise intervention for species with traits considered most sensitive. However, such species may remain highly sensitive to threats even under low levels of threat intensity, requiring almost complete abatement to recover (*e.g.* in the case of slow-living mammals whose population growth is highly sensitive to even small increases in adult mortality) (20, 9). In contrast, species with less sensitive traits at lower intensities, and therefore higher response thresholds to threats, may benefit most from even modest reductions in threat intensity. As a result, we argue that there are contexts under which conservation cost-effectiveness may shift towards less sensitive species, depending on the position of intensity thresholds, and the capacity of threat abatement.

At a broader ecological scale, interactions between trait-mediated response to threats and intensity have consequences for our understanding of future functional diversity loss. The distribution of extinction risk/population declines across trait spaces is often used to highlight regions of global functional diversity and associated ecological services at greatest risk of being lost (3, 29). Our findings emphasise that if anthropogenic threats continue to intensify as forecast (30), patterns of risk across trait spaces may shift substantially. Specifically, we may expect patterns of risk to shift towards those identified under high intensity, resulting in the emergence of new hotspots of risk, or stabilisation of response, depending on position in the trait space. Estimates of functional diversity loss based upon static species sensitivities to decline (*i.e.* models that exclude intensity) may misinterpret regions of the trait space and associated functions genuinely at greatest risk under future conditions. Coupling dynamic, non-stationary estimates of trait-mediated sensitivity, such as those derived in the present analyses, with projections of future threat conditions may provide a pathway to address this challenge.

Whilst our analysis emphasises the existence of trait-threat intensity interactions, several extensions are required to fully explore the limits and implications of this dynamic. First, here we apply population scope, the proportion of a species global population exposed to a threat, as our measure of threat intensity (15). This measure is directly comparable across threat types and taxa, and widely available across many species, making it well-suited to a macroecological comparative study. Population scope is also likely correlated to other metrics of intensity (*e.g.,* species that are hunted across their whole range are more likely to also be under high demand, resulting in greater intensity of hunting practices within the scope of the threat). Indeed, population scope is significantly and positively associated with severity of population response for all threats examined, as expected (see Supplementary Materials: The relationship between threat intensity and population response). Nevertheless, the population scope measures in our analysis remain relatively coarse. Data on threat intensity at greater resolution will be key to support precise reconstructions of response thresholds and demographic tipping points, despite the trade-off with taxonomic and geographic scope. In addition, exploring if and how observed trait-threat intensity interactions shift under different measures of intensity (*e.g.* rate of change or habitat scope) would be a valuable extension of this work, supporting broader applications for policy development, such as in land-sparing *vs*. land-sharing debates (*e.g.* 31).

That trait-based threat-response relationships are non-stationary across intensification gradients poses substantial challenges to the transferability of current trait-based predictions in conservation. However, these findings also offer the opportunity to extend applications of trait-based models in biodiversity forecasts. Specifically, identifying threshold levels of responses to different threats is central to conservation, but limited empirical data presents a serious challenge to the quantification of such relationships for the majority of threatened species (6). Our findings highlight the opportunity to capitalise on the interaction between species traits, threat intensity, and population response to derive estimates of non-linear response curves, and to ground these dynamics in demographic mechanisms. Such approaches could provide valuable contributions to the realism of generalisable biodiversity forecasts, facilitating the incorporation of specific scenarios of threat development, whilst requiring comparatively little empirical data. Reframing trait-mediated sensitivity from a static to a dynamic indicator of species risk challenges current interpretations of trait-based models, but we argue that this development expands rather than limits the potential of traits to inform conservation strategies in a rapidly changing world.

Methods

Data collection and preparation

We compiled an extensive dataset of population responses to threats across bird and mammal species, including threat type, threat intensity, estimated rate of population decline, life history traits, and phylogenetic relationships. The following section details the sources and methods of preparation for each variable. In total, we collected data on traits for 8,497 bird and 3,364 mammal species, and 7,715 bird responses (2,129 species) and 1,547 mammal responses (424 species) across threat types.

Threat response data:

Global comparative studies of species risk across the trait space typically apply extinction risk as a proxy of response to threats (12). Whilst extinction risk is beneficial in its wide availability across species and ease of interpretation, it is a composite measure of species response under all threats across the species range. Thus, whilst most species are exposed to more than one threat (32), extinction risk offers no indication of the degree to which each threat contributes to a species overall response. This issue is particularly important when incorporating threat intensity into models, where

a direct link between independent threat intensities and their associated population responses is required.

Therefore, we used data for the response of populations to distinct threats from the IUCN Red List (15). Most species assessments in the IUCN Red List include a list of identified threats, optionally accompanied by information on threat severity, ranging from negligible to very rapid population decline (hereafter, population response to the threat). We collected data on population response to three broad categories of threat: habitat loss, hunting, and invasive species/disease (see Table 2 for allocation of red list threat classifications). For habitat loss, we considered the following Red List threat classifications: “Residential & Commercial development”, “Agriculture & Aquaculture”, and “Logging & Wood Harvesting”. For hunting, we considered the red list classification “Hunting & Collecting Terrestrial Animals; species being assessed is the target”, excluding unintentional effects of hunting (*e.g.,* due to loss of prey). For invasive species and disease, we considered the Red List classification “Invasive & Other Problematic Species, Genes & Disease”. We categorised the population response variable into three ordered levels: High (causing very rapid declines, or rapid declines); Medium (causing slow but significant declines); and Low (causing fluctuations, negligible, or no declines). We excluded species with no severity information from our analyses. There were insufficient numbers of mammal responses to invasive species/disease with accompanying threat intensity data ($n < 150$ species), so we excluded this threat from our mammal analysis.

Table 2: Threat categorisations defined by Red List threat classes. We collected response data from the IUCN Red List (15) on three key threats: habitat loss, hunting, and invasive species/disease. We grouped responses into broad threat categories based on the Red List threat classification scheme. Where the 1st level threat class is shown in the table below, all sub-threats from this class were included, otherwise sublevels are listed (*e.g.* in hunting, we were only interested in direct harvest (5.1.1) where the species was the target, rather than indirect effects of harvest on other species, such as prey loss).

Threat categorisation	Red List threat classification
Habitat Loss	Residential & Commercial Development (1); Agriculture and Aquaculture (2); Logging & Wood Harvesting, species being assessed is not the target (5.3.3, 5.3.4, 5.3.5)
Hunting	Hunting & Collecting Terrestrial Animals, species being assessed is the target (5.1.1)
Invasive Species/Disease	Invasive & Other Problematic Species, Genes & Diseases (8)

Threat intensity:

Here, we define threat intensity as the proportion of a species' global population exposed to a given threat (hereafter, population scope). We selected population scope to capture threat intensity as it allows direct comparison of intensity levels across threat types and is widely available for many species and threats in the IUCN Red List (15). As with threat severity, population scope is optionally recorded for each threat listed under a species assessment, in the form of a categorical variable: minority (<50% population exposed, hereafter low intensity), majority (50-90% population exposed, hereafter moderate intensity), or whole (>90% population exposed, hereafter high intensity). We extracted the associated population scope for all available population response data. To be included in our analysis, population response data had to be accompanied by an associated measure of population scope (*i.e.* where population scope was unknown, the response was excluded from our analyses).

Life history trait data:

To characterise the life history strategies of species in our dataset, we identified relevant traits with sufficient data availability across species (> 500 species records for each trait). For birds, we selected nine traits: maximum longevity (years), age at sexual maturity (days), egg mass (g), clutch

size, number of clutches per year, incubation time (days), fledgling age (days), adult body mass (g), and snout-vent-length (cm). For mammals, we selected eight traits: maximum longevity (years), age at sexual maturity (days), litter size, number of litters per year, gestation length (days), weaning length (days), adult body mass (g), and adult snout-vent-length (cm). All trait data were collected from the Amniote database (16).

Data for the life history traits of species were incomplete (for details, see Supplementary Materials: Imputing missing life history trait data). To fill in missing values, we used a Multiple Imputation approach via the R package *mice* (33). Multiple imputation (34) has been suggested to impute ecological datasets better than other available approaches by explicitly accounting for variation and error in estimated values (35). The inclusion of phylogenetic information is also known to improve estimations of missing trait values (36). As such, we gathered maximum clade credibility (MCC) phylogenetic trees for birds and mammals (37, 38). Following the author recommendations (38), we used the DNA-only MCC tree for mammals. To represent the evolutionary relationships of our species, we constructed phylogenetic eigenvectors (39). We used the first 10 eigenvectors in our imputation, as recommended by (36). Species not included in the phylogenetic trees could not be assigned eigenvectors and were therefore excluded from our analyses.

Prior to imputation, all traits were log-transformed to conform to normality assumptions. We used predictive mean matching to impute traits (40). To account for uncertainty in the imputation method, we created 60 imputed datasets for birds and 30 datasets for mammals, aligning with the overall proportion of missingness in the respective trait datasets (57.2% in birds, 31.9% in mammals). To assess imputation success, we visualised our imputed datasets with density and convergence plots (for details see Supplementary Materials: Imputing missing life history trait data). Finally, to ensure imputed trait values were biologically plausible, we applied a post-harmonisation function to compress the standard deviation of any given missing trait value across imputations to no more than 25% of the mean across imputations.

Characterising the life history trait space

We performed a Principal Component Analysis (PCA) on our imputed trait data to identify the main axes of variation in the life history strategies of our examined mammals and birds. To support our multiple imputation approach, we produced 60 bird and 30 mammal PCA trait spaces, one for each imputed dataset. To determine the number of axes to retain for the next steps of our analytical

pipeline, we applied a threshold of 75% cumulative variance explained, which resulted in two axes across all imputed datasets, for both bird and mammal trait spaces. Variation in trait data across imputed datasets resulted in small variations in the loadings of the trait spaces between imputations. To pool model results across imputations, the trait spaces between imputed datasets must be directly comparable. We therefore constructed a consensus trait space by aligning PCAs from each imputation via Generalised Procrustes Analysis (41), and for each imputed dataset, reprojected species scores into the consensus space, as suggested by (42, 43, 44). This approach produced 60 and 30 trait spaces for birds and mammals, respectively, with the same loadings, but which retained variation in species scores (*i.e.* species positions in the trait spaces) due to imputation variation. Full loadings of the consensus trait space can be found in Supplementary Tables 1 & 2. For both birds and mammals, to visualise the average distribution of species across our consensus trait spaces, we performed kernel density estimation based on the mean positions of species across imputations, via the R package "funspace" (45) (Figure 1). To estimate the average variance explained by each of our principal components in the consensus trait space, we calculated the mean variance explained for each principal component across imputations. The subsequent analyses were run on each imputed trait-space independently, and results were pooled using Rubin's rules across birds and mammals, respectively (46). All results presented in the main text are the product of pooling across imputations. For further details on PCA construction and the resulting trait spaces, see Supplementary Materials: Bird and mammal life history trait spaces.

Modelling the interaction between threat intensity, life history traits, and population response to threats

To characterise the relationship between threat intensity, life history traits, and population response to our three examined threats, we used Generalised Additive Models (GAMs) with a cumulative logit link, implemented via the ocat family in the mgcv R package (47). Specifically, we subset our mammal and bird datasets according to each broad threat type: habitat loss, hunting, and invasive species/disease. For each threat, we then produced the following model (Equation 1): severity of population response as the response variable, position in life history space as a predictor variable, including an interaction term with threat intensity (three-level ordinal variable: Low, Moderate, and High), and an additional parametric term for threat intensity. Position in the life history space was included as a tensor smooth product representing scores of a species within the consensus trait space (te(PC1, PC2)), following (3). To account for the phylogenetic non-independence of species

within our dataset, we included a phylogenetic penalty in our models via a Markov Random Field smooth term. Since a large portion of species are impacted by more than one threat class within each broad category (*e.g.* a species may be exposed to both deforestation and agricultural land conversion, both of which fall under habitat modification), we included species name as a random effect to account for non-independence. For hunting models, since we considered only one threat class (direct hunting, Red List code: 5.1.1), we did not include species name as a random effect.

Equation 1:

$$Population\ response \sim te(PC1, PC2, by = intensity) + intensity + s(phylo\ penalty) + re(species\ name)$$

To explore how population response to threats varies due to our selected measure of intensity alone, we performed pairwise comparisons of estimated marginal mean responses across the three levels of intensity in each threat model via the R package "emmeans" (48). The log odds ratios of pairwise comparisons from each imputed dataset were pooled according to Rubin's rules (46). Results from this analysis can be found in Supplementary Methods: The relationships between threat intensity and population response.

To examine the interaction between life history traits and threat intensity, we explored how patterns of trait-based sensitivity to each threat varied across increasing levels of intensity. To assess the overall strength of association between traits and population response for each threat at each level of intensity, we pooled the p-values of trait smooths by taking the median p-values across imputations, following (49, 50). To visualise trait effects, for each threat model, we extracted the predicted effect size of our smooth term (te(PC1, PC2)) for each pixel across the trait space at low, moderate, and high intensity, using the predict function in mgcv (47). We completed this across each imputed dataset, and predicted effect sizes were pooled using Rubin's rules (46) (Figures 1 & 2). To avoid extrapolating trait effects beyond the scope of our data, we only visualised estimated trait effects for pixels in the trait space within a threshold distance of the nearest data point (10% of the unit square diagonal away from the nearest observation), according to the average positions of species across imputations (as supported in the gratia R package, 51). Finally, to assess the robustness of trait patterns against error associated with both data imputation and the model itself, we extracted and visualised effect sizes across the trait space at the upper and lower 95% confidence intervals for each threat model (Supplementary Figures 8-12). All analyses were conducted in R version 4.4.1 (52).

References

1. Davidson, A.D. et al. (2017) 'Geography of current and future global mammal extinction risk', PLOS ONE, 12(11), p. e0186934. Available at: https://doi.org/10.1371/journal.pone.0186934.
2. Griffith, P. et al. (2023) 'Using functional traits to identify conservation priorities for the world's crocodylians', Functional Ecology, 37(1), pp. 112–124. Available at: https://doi.org/10.1111/1365-2435.14140
3. Carmona, C.P. et al. (2021) 'Erosion of global functional diversity across the tree of life', Science Advances, 7(13), p. eabf2675. Available at: https://doi.org/10.1126/sciadv.abf2675
4. Bowler, D.E. et al. (2020) 'Mapping human pressures on biodiversity across the planet uncovers anthropogenic threat complexes', People and Nature, 2(2), pp. 380–394. Available at: https://doi.org/10.1002/pan3.10071.
5. Venter, O. et al. (2016) 'Sixteen years of change in the global terrestrial human footprint and implications for biodiversity conservation', Nature Communications, 7(1), p. 12558. Available at: https://doi.org/10.1038/ncomms12558
6. Ingram, D.J. et al. (2021) 'Targeting Conservation Actions at Species Threat Response Thresholds', Trends in Ecology & Evolution, 36(3), pp. 216–226. Available at: https://doi.org/10.1016/j.tree.2020.11.004
7. Pereira, H.M., Navarro, L.M. and Martins, I.S. (2012) 'Global Biodiversity Change: The Bad, the Good, and the Unknown', Annual Review of Environment and Resources, 37(Volume 37, 2012), pp. 25–50. Available at: https://doi.org/10.1146/annurev-environ-042911-093511
8. Dickinson, M.G. et al. (2014) 'Separating sensitivity from exposure in assessing extinction risk from climate change', Scientific Reports, 4(1), p. 6898. Available at: https://doi.org/10.1038/srep06898
9. González-Suárez, M., Gómez, A. and Revilla, E. (2013) 'Which intrinsic traits predict vulnerability to extinction depends on the actual threatening processes', Ecosphere, 4(6), p. art76. Available at: https://doi.org/10.1890/ES12-00380.1
10. Mace, G.M. et al. (2018) 'Aiming higher to bend the curve of biodiversity loss', Nature Sustainability, 1(9), pp. 448–451. Available at: https://doi.org/10.1038/s41893-018-0130-0
11. Balmford, A. et al. (2000) 'Integrating Costs of Conservation into International Priority Setting', Conservation Biology, 14(3), pp. 597–605

12. Chichorro, F., Juslén, A. and Cardoso, P. (2019) 'A review of the relation between species traits and extinction risk', Biological Conservation, 237, pp. 220–229. Available at: https://doi.org/10.1016/j.biocon.2019.07.001
13. Sutherland, W.J. et al. (2013) 'Identification of 100 fundamental ecological questions', Journal of Ecology, 101(1), pp. 58–67. Available at: https://doi.org/10.1111/1365-2745.12025
14. Milles, A. et al. (2023) 'Local buffer mechanisms for population persistence', Trends in Ecology & Evolution, 38(11), pp. 1051–1059. Available at: https://doi.org/10.1016/j.tree.2023.06.006
15. IUCN. 2025. The IUCN Red List of Threatened Species. Version 2025-2. https://www.iucnredlist.org. Accessed March 2025.
16. Myhrvold, N.P. et al. (2015) 'An amniote life-history database to perform comparative analyses with birds, mammals, and reptiles', Ecology, 96(11), pp. 3109–3109. Available at: https://doi.org/10.1890/15-0846R.1.
17. Gaillard, J.-M. et al. (1989) 'An Analysis of Demographic Tactics in Birds and Mammals', Oikos, 56(1), pp. 59–76. Available at: https://doi.org/10.2307/3566088
18. Stearns, S.C. (1977) 'The Evolution of Life History Traits: A Critique of the Theory and a Review of the Data', Annual Review of Ecology and Systematics, 8, pp. 145–171
19. Chichorro, F., Correia, L. and Cardoso, P. (2022) 'Biological traits interact with human threats to drive extinctions: A modelling study', *Ecological Informatics*, 69, p. 101604. Available at: https://doi.org/10.1016/j.ecoinf.2022.101604
20. Heppell, S.S., Caswell, H. and Crowder, L.B. (2000) 'Life Histories and Elasticity Patterns: Perturbation Analysis for Species with Minimal Demographic Data', *Ecology*, 81(3), pp. 654–665. Available at: https://doi.org/10.1890/0012-9658(2000)081%255B0654:LHAEPP%255D2.0.CO;2.
21. Fowler, C.W. (1987) 'A Review of Density Dependence in Populations of Large Mammals', in H.H. Genoways (ed.) *Current Mammalogy*. Boston, MA: Springer US, pp. 401–441. Available at: https://doi.org/10.1007/978-1-4757-9909-5_10
22. Payo-Payo, A. *et al.* (2015) 'Population control of an overabundant species achieved through consecutive anthropogenic perturbations', *Ecological Applications*, 25(8), pp. 2228–2239. Available at: https://doi.org/10.1890/14-2090.1

23. Doak, D.F. and Morris, W.F. (2010) 'Demographic compensation and tipping points in climate-induced range shifts', *Nature*, 467(7318), pp. 959–962. Available at: https://doi.org/10.1038/nature09439

24. Rodríguez-Caro, R.C. *et al.* (2021) 'The limits of demographic buffering in coping with environmental variation', *Oikos*, 130(8), pp. 1346–1358. Available at: https://doi.org/10.1111/oik.08343

25. Melo, I. et al. (2018) 'A review of threshold responses of birds to landscape changes across the world', Journal of Field Ornithology, 89(4), pp. 303–314. Available at: https://doi.org/10.1111/jofo.12272

26. Cayuela, H. *et al.* (2022) 'Compensatory recruitment allows amphibian population persistence in anthropogenic habitats', *Proceedings of the National Academy of Sciences*, 119(38), p. e2206805119. Available at: https://doi.org/10.1073/pnas.2206805119

27. Galic, N. *et al.* (2024) 'Ecological risk assessment when species-specific data are scarce: how trait-based approaches and modeling can help', *BioScience*, 74(10), pp. 701–709. Available at: https://doi.org/10.1093/biosci/biae086

28. Cazalis, V. *et al.* (2022) 'Bridging the research-implementation gap in IUCN Red List assessments', *Trends in Ecology & Evolution*, 37(4), pp. 359–370. Available at: https://doi.org/10.1016/j.tree.2021.12.002

29. Rodríguez-Caro, R.C. *et al.* (2023) 'Anthropogenic impacts on threatened species erode functional diversity in chelonians and crocodilians', *Nature Communications*, 14(1), p. 1542. Available at: https://doi.org/10.1038/s41467-023-37089-5

30. Steffen, W. et al. (2015) 'The trajectory of the Anthropocene: The Great Acceleration', The Anthropocene Review, 2(1), pp. 81–98. Available at: https://doi.org/10.1177/2053019614564785

31. Phalan, B. et al. (2011) 'Reconciling Food Production and Biodiversity Conservation: Land Sharing and Land Sparing Compared', Science, 333(6047), pp. 1289–1291. Available at: https://doi.org/10.1126/science.1208742.

32. Capdevila, P. *et al.* (2025) 'Halting predicted vertebrate declines requires tackling multiple drivers of biodiversity loss'. bioRxiv, p. 2025.01.02.630023. Available at: https://doi.org/10.1101/2025.01.02.630023

33. Buuren, S. van and Groothuis-Oudshoorn, K. (2011) 'mice: Multivariate Imputation by Chained Equations in R', *Journal of Statistical Software*, 45, pp. 1–67. Available at: https://doi.org/10.18637/jss.v045.i03
34. Rubin, D.B. (1976) 'Inference and missing data', *Biometrika*, 63(3), pp. 581–592. Available at: https://doi.org/10.1093/biomet/63.3.581
35. Blomberg, S.P. and Todorov, O.S. (2025) 'The fallacy of single imputation for trait databases: Use multiple imputation instead', *Methods in Ecology and Evolution*, 16(4), pp. 658–667. Available at: https://doi.org/10.1111/2041-210X.14494.
36. Penone, C. *et al.* (2014) 'Imputation of missing data in life-history trait datasets: which approach performs the best?', *Methods in Ecology and Evolution*, 5(9), pp. 961–970. Available at: https://doi.org/10.1111/2041-210X.12232
37. McTavish, E.J. et al. (2025) 'A complete and dynamic tree of birds', Proceedings of the National Academy of Sciences, 122(18), p. e2409658122. Available at: https://doi.org/10.1073/pnas.2409658122.
38. Upham, N.S., Esselstyn, J.A. and Jetz, W. (2019) 'Inferring the mammal tree: Species-level sets of phylogenies for questions in ecology, evolution, and conservation', PLOS Biology, 17(12), p. e3000494. Available at: https://doi.org/10.1371/journal.pbio.3000494.
39. Diniz-Filho, J.A.F., Sant'Ana, C.E.R. de and Bini, L.M. (1998) 'An eigenvector method for estimating phylogenetic inertia', *Evolution*, 52(5), pp. 1247–1262. Available at: https://doi.org/10.1111/j.1558-5646.1998.tb02006.x
40. Van Buuren, S. (2018). *Flexible Imputation of Missing Data. Second Edition.* Chapman & Hall/CRC. Boca Raton, FL. Available at: https://stefvanbuuren.name/fimd/sec-pmm.html
41. Gower, J.C. and Dijksterhuis, G.B. (2004) *Procrustes Problems*. OUP Oxford
42. van Ginkel, J.R. and Kroonenberg, P.M. (2014) 'Using Generalized Procrustes Analysis for Multiple Imputation in Principal Component Analysis', Journal of Classification, 31(2), pp. 242–269. Available at: https://doi.org/10.1007/s00357-014-9154-y
43. Josse, J., Pagès, J. and Husson, F. (2011) 'Multiple imputation in principal component analysis', Advances in Data Analysis and Classification, 5(3), pp. 231–246. Available at: https://doi.org/10.1007/s11634-011-0086-7
44. van Ginkel, J.R. (2023) 'Handling Missing Data in Principal Component Analysis Using Multiple Imputation', in L.A. van der Ark, W.H.M. Emons, and R.R. Meijer (eds) Essays on

Contemporary Psychometrics. Cham: Springer International Publishing, pp. 141–161. Available at: https://doi.org/10.1007/978-3-031-10370-4_8

45. Carmona, C.P., Pavanetto, N. and Puglielli, G. (2024) 'funspace: An R package to build, analyse and plot functional trait spaces', *Diversity and Distributions*, 30(4), pp. 1–14
46. Barnard, J. and Rubin, D. (1999) 'Miscellanea. Small-sample degrees of freedom with multiple imputation', *Biometrika*, 86(4), pp. 948–955. Available at: https://doi.org/10.1093/biomet/86.4.948
47. *Mixed GAM Computation Vehicle with GCV/AIC/REML smoothness estimation and GAMMs by REML/PQL - R Documentation*. Available at: https://www.typeerror.org/docs/r/library/mgcv/html/mgcv-package
48. Lenth, R.V. et al. (2025) 'emmeans: Estimated Marginal Means, aka Least-Squares Means'. Available at: https://cran.r-project.org/web/packages/emmeans/index.html
49. Eekhout, I., van de Wiel, M.A. and Heymans, M.W. (2017) 'Methods for significance testing of categorical covariates in logistic regression models after multiple imputation: power and applicability analysis', BMC Medical Research Methodology, 17(1), p. 129. Available at: https://doi.org/10.1186/s12874-017-0404-7
50. Bolt, M.A. et al. (2022) 'Inference following multiple imputation for generalized additive models: an investigation of the median p-value rule with applications to the Pulmonary Hypertension Association Registry and Colorado COVID-19 hospitalization data', BMC Medical Research Methodology, 22(1), p. 148. Available at: https://doi.org/10.1186/s12874-022-01613-w.
51. Simpson, G.L. and Singmann, H. (2026) 'gratia: Graceful 'ggplot'-Based Graphics and Other Functions for GAMs Fitted Using "mgcv"'. Available at: https://cran.r-project.org/web/packages/gratia/index.html (Accessed: 3 April 2026).
52. R Core Team (2024). R: A Language and Environment for Statistical Computing. R Foundation for Statistical Computing, Vienna, Austria. Available at: https://www.R-project.org

Supplementary Materials

Threat intensification reshapes trait-response relationships in birds and mammals

Index

Bird and mammal life history trait spaces

To define the life history trait spaces for species within our dataset, we conducted a principal component analysis (PCA) on nine key life history traits in birds and eight in mammals. As trait data are incomplete for many species, we applied a novel imputation approach during principal component analysis, allowing us to propagate uncertainty from missing trait values into downstream analyses. To retain the variation and associated error captured by multiply imputed trait values, we constructed independent PCA trait spaces for each imputed dataset (60 for birds, 30 for mammals). Due to variations in trait values across imputations, loading values varied across trait spaces from each imputed dataset. To pool model results across imputed datasets, the scale of each trait space must be directly comparable; i.e., the loadings must be identical across imputed datasets. To allow direct comparisons across trait spaces between imputed datasets, we produced a consensus trait space by aligning PCAs from each imputation via Generalised Procrustes Analysis (1), following (2, 3, 4). Species scores from each imputed dataset were re-projected into the trait consensus space. This resulted in a set of trait spaces for birds and mammals with identical loadings, but with distinct species scores according to variations in imputed trait values for each imputed dataset. To estimate the average

variance explained by our consensus axes, we calculated the mean variance explained for each axis across imputations. Loadings and estimated variance explained for the first two principal components in the consensus trait space are shown in Supplementary Tables 1 (birds) and 2 (mammals). Subsequent analyses were performed on species scores in the consensus space from each imputation independently and pooled via Rubin's rules to produce final results. This approach enabled our model confidence intervals to reflect both the uncertainty due to variation in imputed values, as well as general model uncertainty.

The resulting trait spaces remain in agreement with the wider literature (*e.g.,* 5) (Supplementary Figure 1). For birds (Supplementary Figure 1A), the majority of variation in life history strategies exists across a diagonal axis, which broadly reflects the fast-slow continuum (6, 7), with both axes representing trade-offs between reproductive output against developmental pace and size-associated traits. Specifically, the first axis (PC1: 67.0%) reflects a trade-off between annual reproductive output (primarily clutches per year and, to a lesser extent, clutch size) against both size-associated traits (body mass, snout-vent-length, and egg mass) and developmental pace (age at maturity, fledgling age, maximum longevity, and incubation length). Slow-paced, large-bodied species occupy high scores along PC1, whilst fast-paced, small-bodied species occupy lower scores. The second axis (PC2: 13.3%) is dominated by an additional trade-off between clutch size and age at maturity. Higher scores along PC2 are associated with later ages of maturity and smaller clutch sizes, whilst lower scores are associated with fast-maturing species with larger clutch sizes. In mammals (Supplementary figure 1B), the first axis of the trait space (PC1: 66.8%) largely reflects the fast-slow continuum (6, 7), and to a weaker extent, species body size, with higher scores associated with longer lifespans, later ages of maturity, slower reproductive strategies (*i.e.*, fewer litters per year and smaller litter size, but with longer gestation and weaning lengths), and larger body sizes. The second axis (PC2, 15.2%) captures an additional trade-off between body size and litter size against developmental pace. Higher scores along PC2 reflect mammal species with larger body sizes but with relatively large litters and fast developmental paces (*e.g.,* hares), whilst lower scores reflect species with smaller body sizes yet smaller litters and slower developmental paces (*e.g.,* bats). Full loadings can be found in Supplementary Tables 1 & 2.

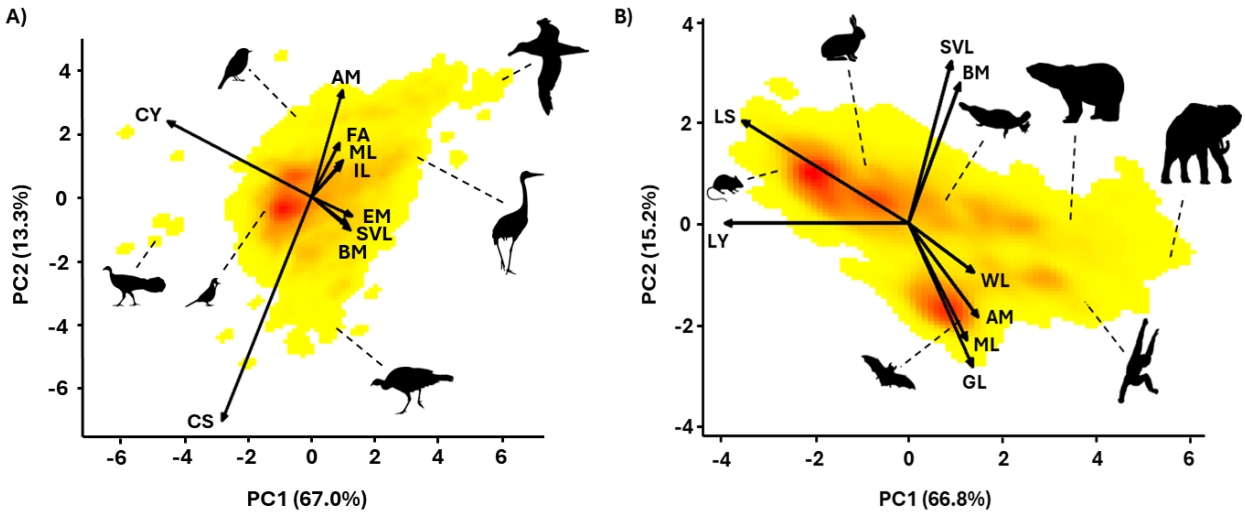

Supplementary Figure 1: Most of the variation in life history strategies across birds and mammals can be described by two key axes of trait variation. Trait density profiles describing the occupation of (A) the examined 8,497 bird species and (B) 3,364 mammal species within their life history trait spaces, defined by the first two principal component axes of a principal component analysis (PCA). The proportion of trait variation explained is shown for each axis. Red colour represents regions of higher species density, while yellow represents lower density. Traits for birds include: maximum longevity (ML; years), age of maturity (AM; days), clutch size (CS), clutches per year (CY), incubation length (IL; days), fledgling age (FA; days), egg mass (EM; grams), adult body mass (BM; grams), and adult snout-vent length (SVL; cm). Traits for mammals include: maximum longevity (ML; years), age of maturity (AM; days) litter size (LS), litters per year (LY), gestation length (GL; days), weaning length (WL; days), adult body mass (BM; g), and adult snout-vent length (SVL; cm). Arrows represent the direction and weighting of each life history trait in the PCA space (for full loadings see Supplementary Tables 1 & 2). For birds (A) silhouettes correspond to (starting from top right and moving clockwise): Tristan albatross (*Diomedea dabbenena*), Red-Crowned Crane (*Grus Japonensis*), Wild turkey (*Meleagris gallopavo*), White-eared bulbul (*Pycnonotus leucotis*), Australian brushturkey (*Alectura lathami*), and Lemon-bellied flyrobin (*Microeca flavigaster*). For mammals (B) silhouettes correspond to (starting from top right and moving clockwise): Platypus (*Ornithorhynchus anatinus*), Polar bear (*Ursus maritimus*), African bush elephant (*Loxodonta africana*), Yellow-cheeked gibbon (*Nomascus gabriellae*), Bechstein's bat (*Myotis bechsteinii*), House mouse (*Mus musculus*), and Snowshoe hare (*Lepus americanus*). All silhouettes were downloaded from PhyloPic (www.phylopic.org).

Supplementary table 1: Consensus loadings and variance explained for the bird trait space. Loadings and mean variance explained (cumulative and total) for the first two principal components of the bird consensus trait space. We also show the symbol used in the main text for each trait.

Trait	Symbol	PC1	PC2
Body mass (g)	BM	0.137	-0.118
Snout-vent length (cm)	SVL	0.129	-0.100
Max longevity (years)	ML	0.110	0.129
Age at maturity (days)	AM	0.110	0.379
Clutch size	CS	-0.321	-0.798
Clutches/y	CY	-0.515	0.269
Egg mass (g)	EM	0.144	-0.068
Incubation length (days)	IL	0.106	0.116
Fledgling age (days)	FA	0.099	0.191
Average variance explained		67.0%	13.3%
Average cumulative variance		67.0%	80.3%

Supplementary Table 2: Consensus loadings and variance explained for the mammal trait space. Loadings and mean variance explained (cumulative and total) for the first two principal components of the mammal consensus trait space. We also show the symbol used in the main text for each trait.

Trait	Symbol	PC1	PC2
Body mass (g)	BM	0.153	0.389
Snout-vent length (cm)	SVL	0.127	0.450
Max longevity (years)	ML	0.173	-0.326
Age at maturity (days)	AM	0.207	-0.262
Litter size	LS	-0.497	0.284
Litters/y	LY	-0.549	0.000
Gestation length (days)	GL	0.191	-0.399
Weaning length (days)	WL	0.194	-0.137
Average variance explained		66.8%	15.2%
Average cumulative variance		66.8%	82.0%

The relationship between threat intensity and population response

The average severity of population response to a threat (here, estimated rate of population decline, 8) is strongly associated with our selected measure of threat intensity (proportion of global population exposed to threat). To assess how population responses to each threat vary due to intensity alone, we compared the average severity of population response between each level of intensity, for all threat models (pairwise comparisons of marginal means, Supplementary Table 3). In all threats, for both birds and mammals, population responses become more severe with increasing levels of threat intensity ($p < 0.01$ in all models for low-high intensity comparison, Supplementary Table 3). However, there is considerable variation in the shape and strength of intensity-response relationships depending on taxa, threat type, and the degree of intensification.

Supplementary Table 3: The average population response becomes more severe with increasing threat intensity. Results of pairwise contrasts of estimated marginal means (log-odds ratios) for severity of population response to threats between increasing levels of intensity, in all threat models for birds and mammals. We compared the average severity of population response between low to moderate, low to high, and moderate to high intensity. We applied a Tukey adjustment to control for multiple comparisons. Standard errors are for each coefficient are shown in parentheses, and statistical significance is shown as follows: * $p < 0.05$, ** $p < 0.01$, *** $p < 0.001$.

	Intensity		
	Low-moderate	Low-high	Moderate-high
Birds			
Habitat modification	1.55 (0.201) ***	4.31 (0.909) **	2.77 (0.903)**
Hunting	2.25 (0.219) ***	3.51 (0.577) ***	1.26 (0.584)*
Invasive species	1.38 (0.279) ***	1.87 (0.443)***	0.488 (0.479)
Mammals			
Habitat modification	1.99 (0.290) ***	3.90 (0.754) ***	1.91 (0.759) *
Hunting	1.69 (0.318) ***	3.18 (0.686) ***	1.49 (0.651) *

The effect of threat intensification on population responses is generally stronger in birds than in mammals. For instance, the odds of a bird species exhibiting a higher severity of response to habitat modification are 74 times greater when the species is exposed to high compared to low intensity (Supplementary Table 3, log odds ratio: 4.31, p = 2.09e-6). For mammal species under the same threat, the odds of a more severe response are around 49 times as great at high *vs.* low intensity (Supplementary Table 3, log odds ratio:

3.90, p = 2.39e-7). Bird species also exhibit greater increases in average responses between low and high intensity of hunting than mammals, although the difference is smaller (Supplementary Table 3, Birds: log odds ratio: 3.51, odds ratio: 33.4, p = 1.27e-09; Mammals: log odds ratio: 3.18, odds ratio: 24.0, p = 3.60e-6). For both birds and mammals, the effect of threat intensification on response between low and high intensity is strongest for habitat modification (Supplementary Table 3, Birds: log odds ratio: 4.31, p = 2.09e-6; Mammals: log odds ratio: 3.90, p = 2.39e-7), followed by hunting (Supplementary Table 3, Birds: log odds ratio: 3.51, odds ratio: 33.4, p = 1.27e-9; Mammals: log odds ratio: 3.18, odds ratio: 24.0, 3.60e-6). For bird species, responses to invasive species and disease show the weakest relationship to intensification from low to high intensity (Supplementary Table 3, log odds ratio: 1.87, 2.49e-5).

The relationship between threat intensity and population response also varies with the degree of threat intensification. Under some threats, the effect of intensification on population responses plateaus with increasing intensity. For instance, in bird responses to invasive species and disease, there is a significant increase in severity of response between low and moderate intensity (Supplementary Table 3, log odds: 1.38, p = 7.76e-7), but no significant change in responses between moderate to high intensity (Supplementary Table 3, p = 0.308). A reduction in threat intensity effects between moderate to high intensity is observed in bird responses to hunting (Supplementary Table 3, low-moderate, log odds: 2.25, p < 1e-16; moderate-high, log odds: 1.26, p = 0.0313), and to a lesser extent, mammal responses to hunting (Supplementary Table 3, low-moderate, log odds: 1.69, p = 1.02e-7; moderate-high, log odds: 1.49, p = 0.0225). The plateau may be associated with a saturation of population response severity. If the majority of species are already experiencing strong declines under moderate threat intensities, further intensification will make increasingly marginal differences in average species response. Indeed, exponentially declining relationships between threat intensity and biodiversity responses have been documented across various systems (*e.g.* in agricultural intensification, 9). A reduction in intensity effects may also be related to stabilisation of population responses at higher intensification following initial declines. These dynamics may be expected where buffering mechanisms reduce fitness but remain effective even under higher levels of threat intensity. For example, a common initial response to disturbance in bird species is dispersal across the species' range. Wider dispersal reduces reproductive output in several species (10, 11) but may buffer isolated populations from rapid declines, even at high intensity of threat (12).

Imputing missing life history trait data

To characterise the life history trait space for birds and mammals, we extracted data on key life history traits for bird and mammal species from the Amniote Life History Database (13). The Amniote database contains life history data for over 21,000 bird, mammal, and reptile species, compiled from peer-reviewed literature, published books, and other existing databases. For our analyses, we selected relevant life history traits from the Amniote database with at least 500 species records for each trait in birds and mammals, respectively. For birds, this selection included nine traits: maximum longevity (years), age at sexual maturity (days), egg mass (g), clutch size, number of clutches per year, incubation time (days), fledgling age (days), adult body mass (g), and snout-vent-length (cm). For mammals, we selected eight traits: maximum longevity (years), age at sexual maturity (days), litter size, number of litters per year, gestation length (days), weaning length (days), adult body mass (g), and adult snout-vent-length (cm). Species for which none of the selected traits was available were excluded from analysis. Since phylogenetic relationships were required for further analyses (including missing data imputation), species with no phylogenetic information were also excluded. Our final trait dataset included 8,497 bird species and 3,364 mammal species.

Life history trait data remained incomplete for both birds (57.2% total missingness) and mammals (31.9% total missingness). The full patterns of trait missingness are shown in Supplementary Figures 2 & 3 for birds and mammals, respectively, visualised via the R package “visdat” (14). The trait with the greatest proportion of missing data for birds was age at sexual maturity (87% missing) followed by adult snout-vent-length (83% missing). In mammals, the traits with the greatest proportion of missing values were age at sexual maturity and length of weaning (53% missing for both traits). Body mass was the most complete trait in both birds (3% missingness) and mammals (4% missingness), followed by clutch size in birds (29% missingness) and adult snout-vent length (17% missing) in mammals.

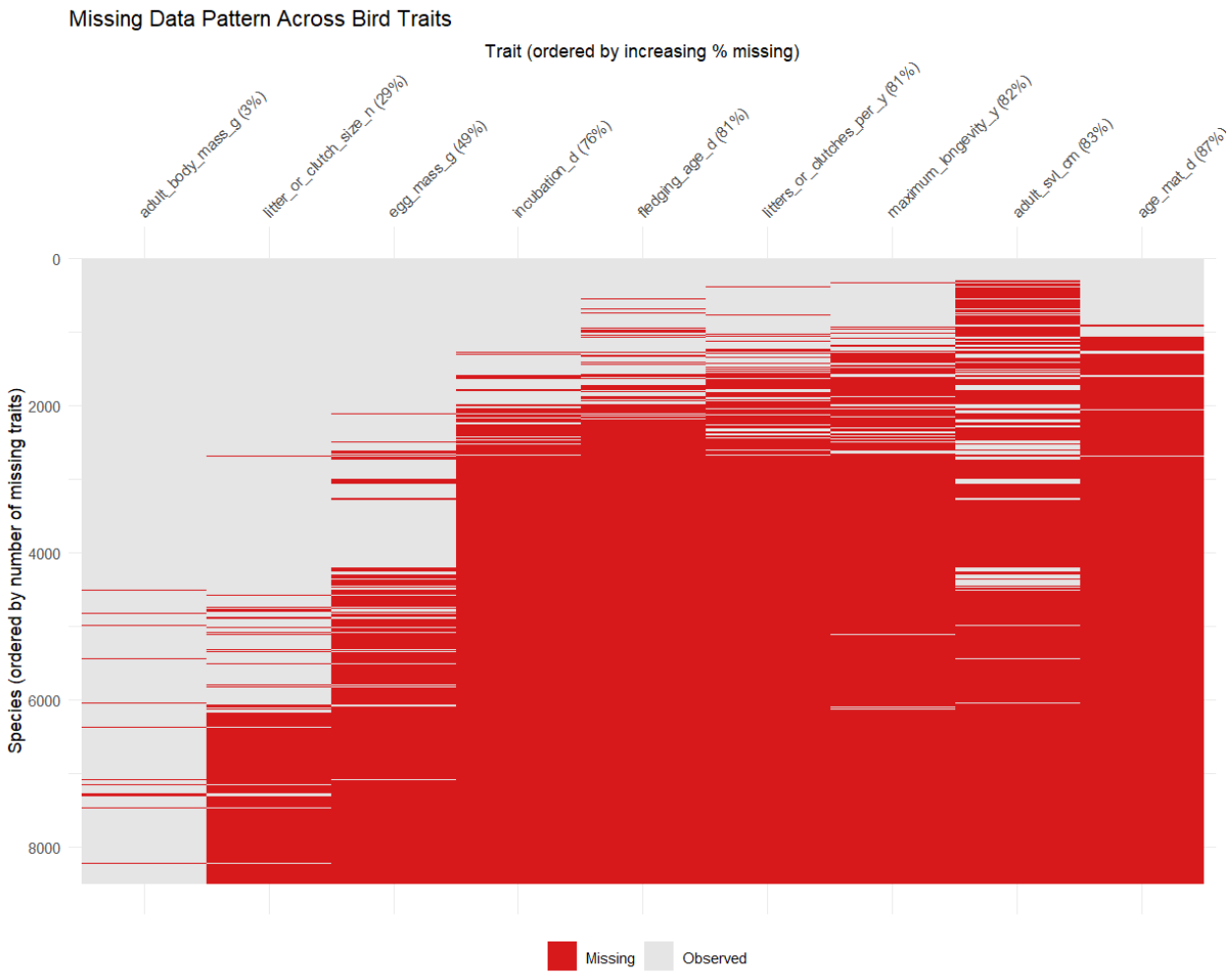

590

591 **Supplementary Figure 2: Patterns of missingness in bird life history data.** We visualised the proportion of
592 missing life history trait data for all species in our life history trait dataset. Life history traits are shown across
593 the x-axis, in order of missingness from least (left) to most (right) missing. Species are shown along the y-axis,
594 in order of missing traits from least (top) to most (bottom) missing. Red bars represent missing trait values;
595 grey bars represent available trait values. Life history traits include (from least to most missing): Body mass
596 (g), clutch size, egg mass (g), incubation length (days), fledgling age (days), clutches per year, maximum
597 longevity (years), adult snout-vent length (cm), and age at sexual maturity (days). In total, we collected data
598 for 8,497 bird species. Total missingness across all traits is 57.2%.

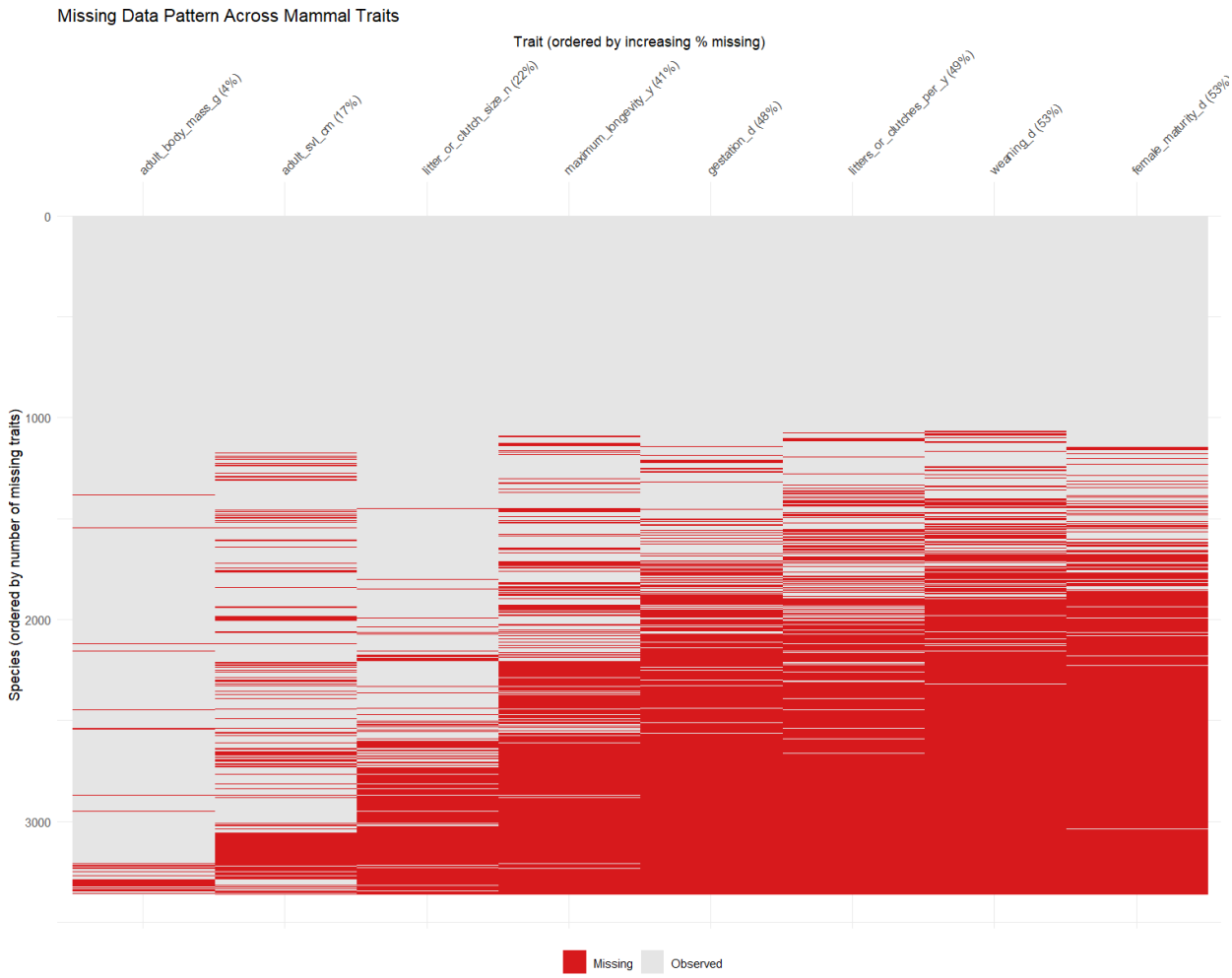

Supplementary Figure 3: Patterns of missingness in mammal life history data. We visualised the proportion of missing life history trait data for all species in our life history trait dataset. Life history traits are shown across the x-axis, in order of missingness from least (left) to most (right) missing. The percentage of missingness for each trait is shown in axis labels. Species are shown along the y-axis, in order of missing traits from least (top) to most (bottom) missing. Red bars represent missing trait values; grey bars represent available trait values. Life history traits include (from least to most missing): body mass (g), adult snout-vent length (cm), litter size, maximum longevity (years), gestation length (days), litters per year, weaning length (days), age at sexual maturity (days). In total, we collected data for 3,364 mammal species. Total missingness across all traits is 31.9%.

As principal component analysis requires complete data, we used multiple imputation to fill in missing life history trait values. We selected a multiple imputation approach (rather than single imputation) as it allows for the explicit consideration of variation and error in imputed values in downstream analysis, rather than treating imputed values as true data (15). All traits were log-10 transformed prior to imputations to conform with normality assumptions. Imputations were carried out on bird and mammal datasets separately, via the R package *mice* (16), using the predictive mean matching method. To assess whether imputations reached convergence, we visually examined convergence plots for each trait in bird and mammal imputations (Supplementary Figures 4 & 5).

To ensure imputed values remained biologically realistic, we applied a post-harmonisation function on imputed datasets to compress the standard deviation of missing trait values in any given imputation to no greater than 25% of the mean trait value across all imputations (for the given species). Specifically, where an imputed trait value for a given species exceeded the 25% variance threshold, it was resampled via predictive mean matching until it fell within the variance threshold. If, after 1000 resampling attempts, a trait value in any given imputation remained outside of the variance threshold, it was assigned the mean trait value across imputations. This harmonisation approach enabled us to retain variation in imputed values (as is the purpose of multiple imputation), whilst ensuring all values fell within biological feasibility for any given species. To compare the distribution of trait values in the original dataset (complete values only) to that in the imputed dataset, and the harmonised imputed dataset, we used density plots (Supplementary Figures 6 & 7). Visually, there was good alignment between trait values in original versus imputed datasets, except for snout-vent length in bird species. Discrepancy between trait values in snout-vent length is likely associated with the high missingness (63%) of data for this trait in birds, potentially combined with a bias in data availability towards larger species (due to difficulties measuring this data for smaller species), such that the average body mass in the imputed datasets is lower than that in the original dataset. Importantly, there was good alignment in trait distributions between original and imputed datasets for body mass, which had substantially less missingness in birds than snout-vent length (3% versus 83% missingness). Thus, we are satisfied that imputations are not systematically underestimating species size (and associated snout-vent length) in our imputed datasets.

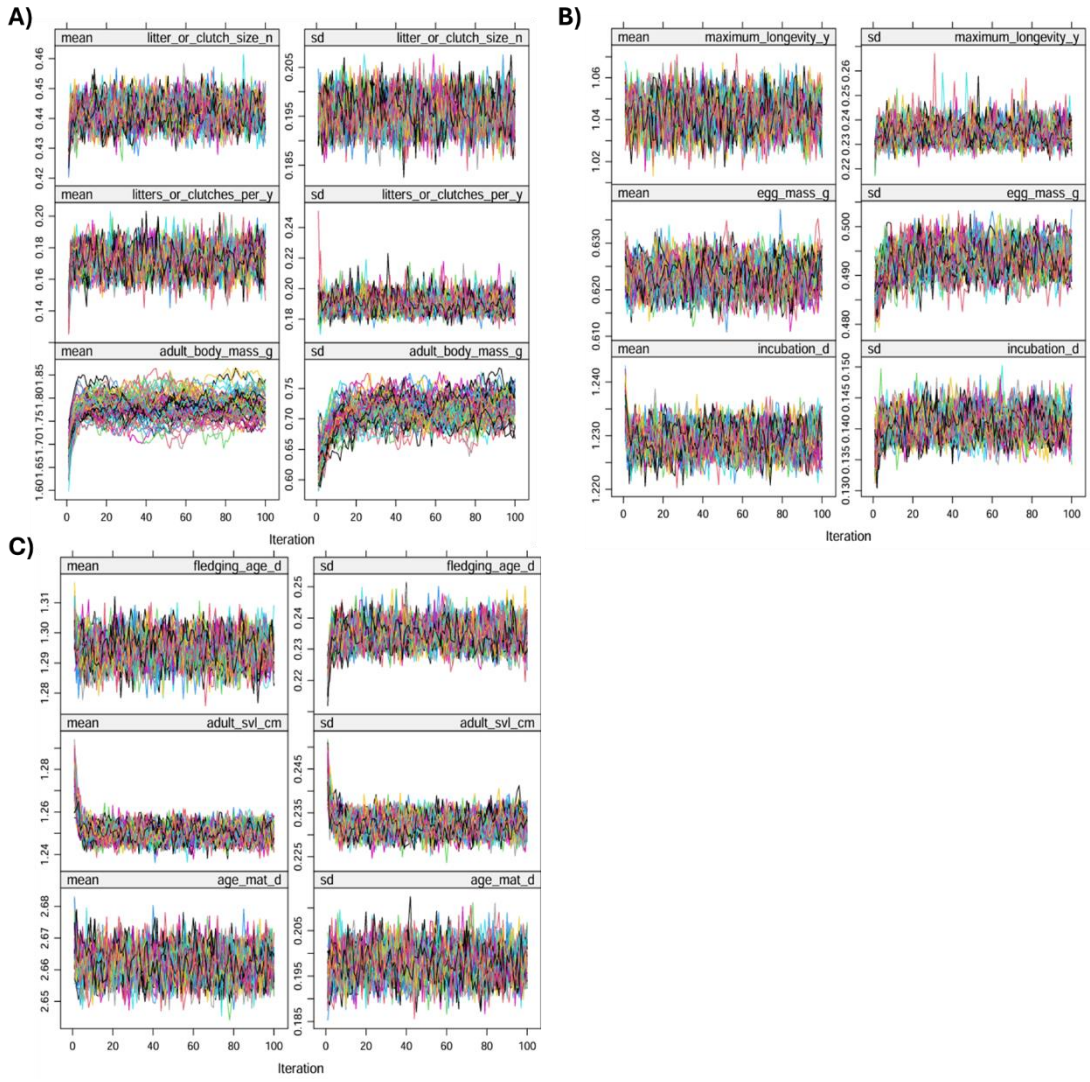

Supplementary Figure 4: Convergence plots for bird trait imputations via MICE. Coloured lines represent for each imputation (60 total imputations) the mean (left panels) and standard deviation (right panels) of imputed values in each trait across 100 iterations for the following traits: A) clutch size, clutches per year, and body mass; B) maximum longevity, egg mass, and incubation length; C) fledgling age, adult snout-vent length, and age at sexual maturity. All traits are log-10 transformed. Across all traits, lines exhibit substantial mixing indicating good convergence.

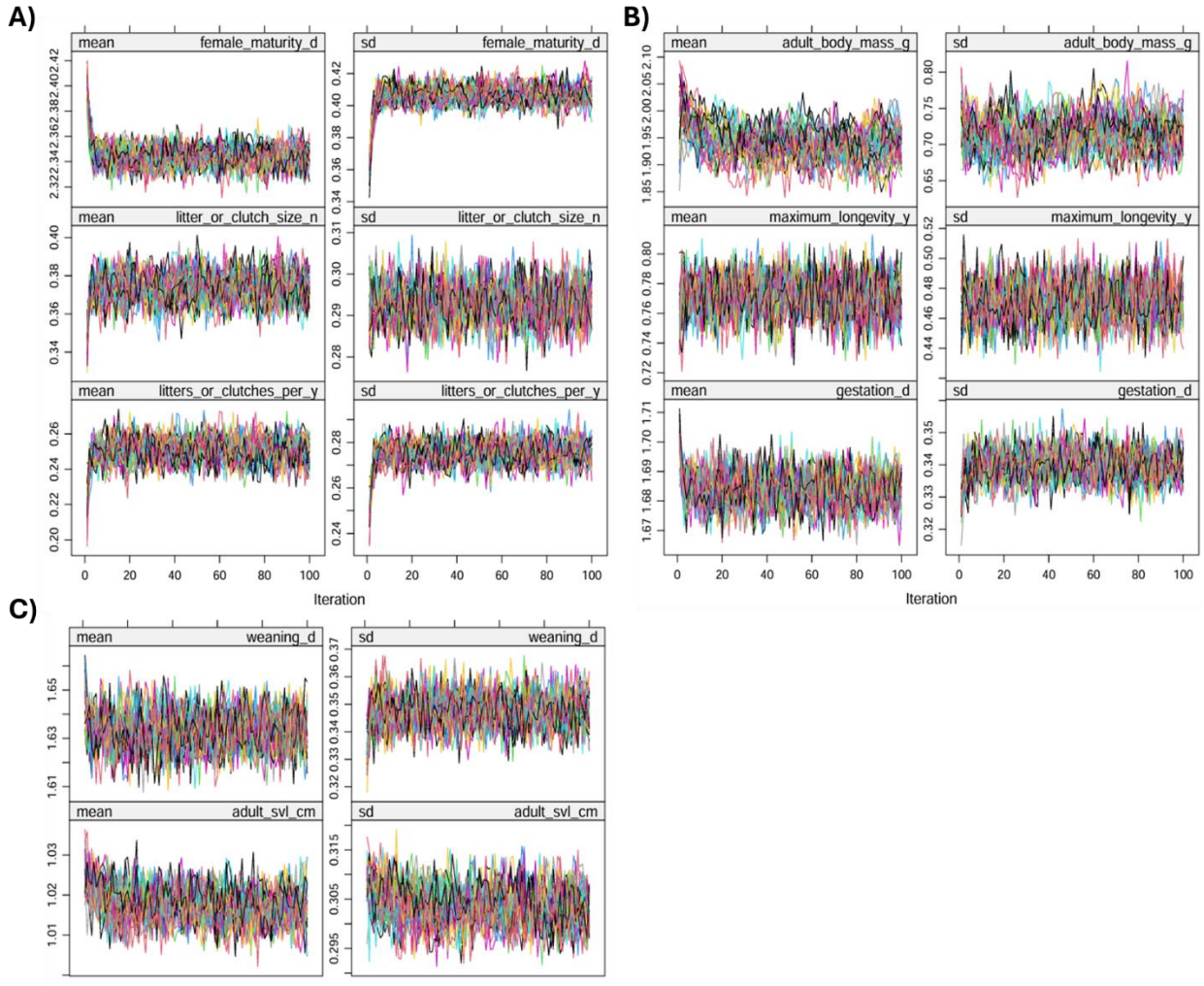

644 **Supplementary Figure 5: Convergence plots for mammal trait imputations via MICE.** Coloured lines
645 represent for each imputation (30 total imputations) the mean (left panels) and standard deviation (right
646 panels) of imputed values in each trait across 100 iterations for the following traits: A) age of sexual maturity,
647 litter size, and litters per year; B) body mass, maximum longevity, and gestation length; C) weaning length,
648 and adult snout-vent length. All trait values are log-10 transformed. Across all traits, lines exhibit substantial
649 mixing indicating good convergence.

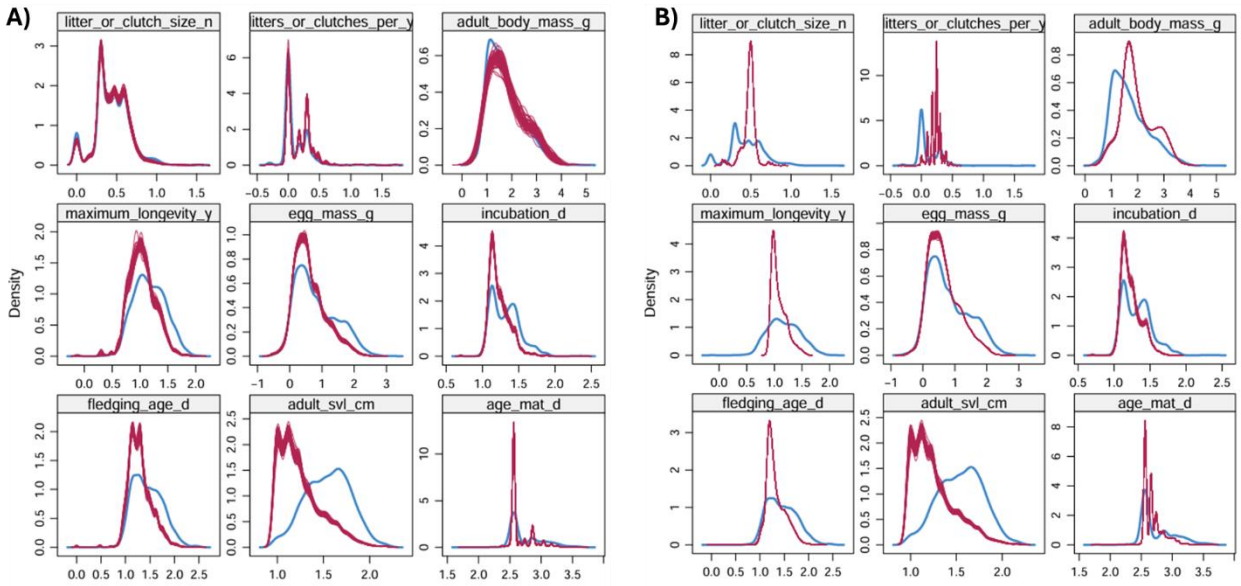

Supplementary Figure 6: Density plots for the distribution of trait values in imputed bird traits (A) pre-harmonisation and (B) post-harmonisation, *versus* original (non-imputed) trait values. In each plot the distribution of trait values in each imputation (red lines, 60 total imputations) is plotted against the distribution of trait values in the original (non-imputed) data (blue line). Panel A shows the data distribution of imputed data prior to harmonisation, and panel B shows the distribution of data post-harmonisation (for details on harmonisation, see "supplementary methods: Imputing missing life history data"). Traits are listed as follows: clutch size, clutches per year, body mass (g), maximum longevity (years), egg mass (g), incubation length (days), fledgling age (days), adult snout-vent length (cm), and age at sexual maturity (days). All trait values are log-10 transformed.

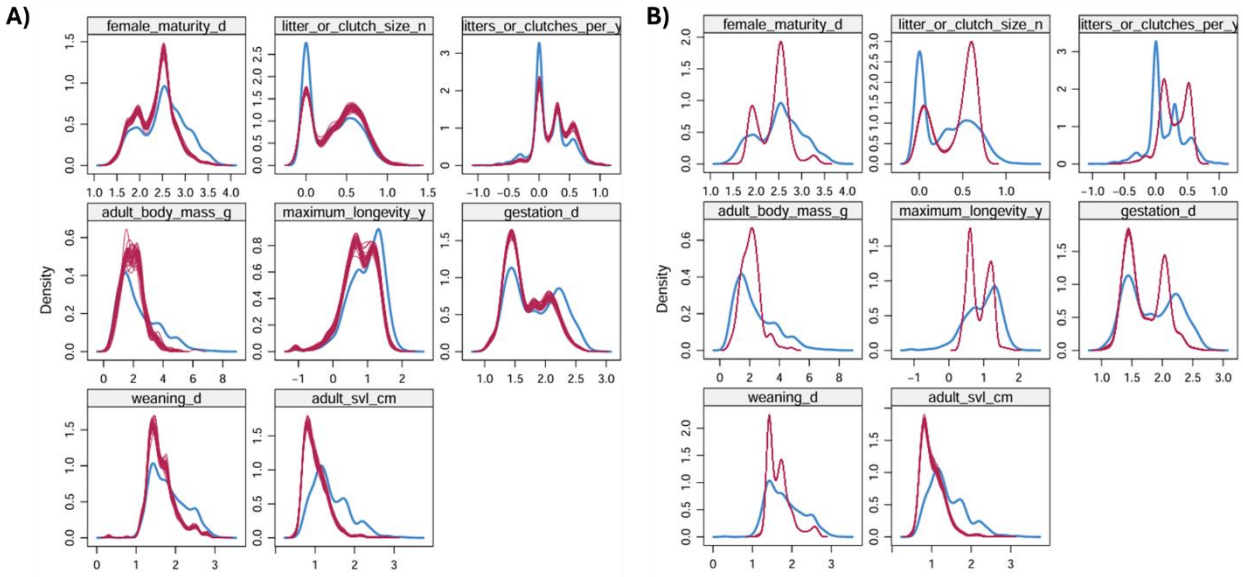

Supplementary Figure 7: Density plots for the distribution of trait values in imputed mammal trait datasets (A) pre-harmonisation and (B) post-harmonisation, *versus* original (non-imputed) trait values. In each plot the distribution of trait values in each imputation (red lines, 30 total imputations) is plotted against the distribution of trait values in the original (non-imputed) data (blue line). Panel A shows the data distribution of imputed data prior to harmonisation, and panel B shows the distribution of imputed data post-harmonisation (for details on harmonisation, see "supplementary methods: Imputing missing life history data"). Traits are listed as follows: age at sexual maturity (d), litter size, litters per year, body mass (g), maximum longevity (years), gestation length (days), weaning length (days), and adult snout-vent length (cm). All trait values are log-10 transformed.

Trait effect confidence intervals

To examine whether trait effects across threat models were robust to model uncertainty, we extracted trait effects at lower and upper 95% confidence intervals for all pixels across the life history trait space (Supplementary Figures 8-12). All patterns discussed in the main text remain robust within the confidence intervals of models. Nevertheless, regions of the trait space with lower species occupancy, and therefore with lower data availability (generally towards the edges of the trait space), show considerable variation in trait effects between confidence intervals. Thus, we caution that trait effects should be interpreted with consideration of data distribution and of confidence intervals shown below. To support this interpretation, data distribution across the trait space are shown for each threat model in the main text (Figures 1 & 2).

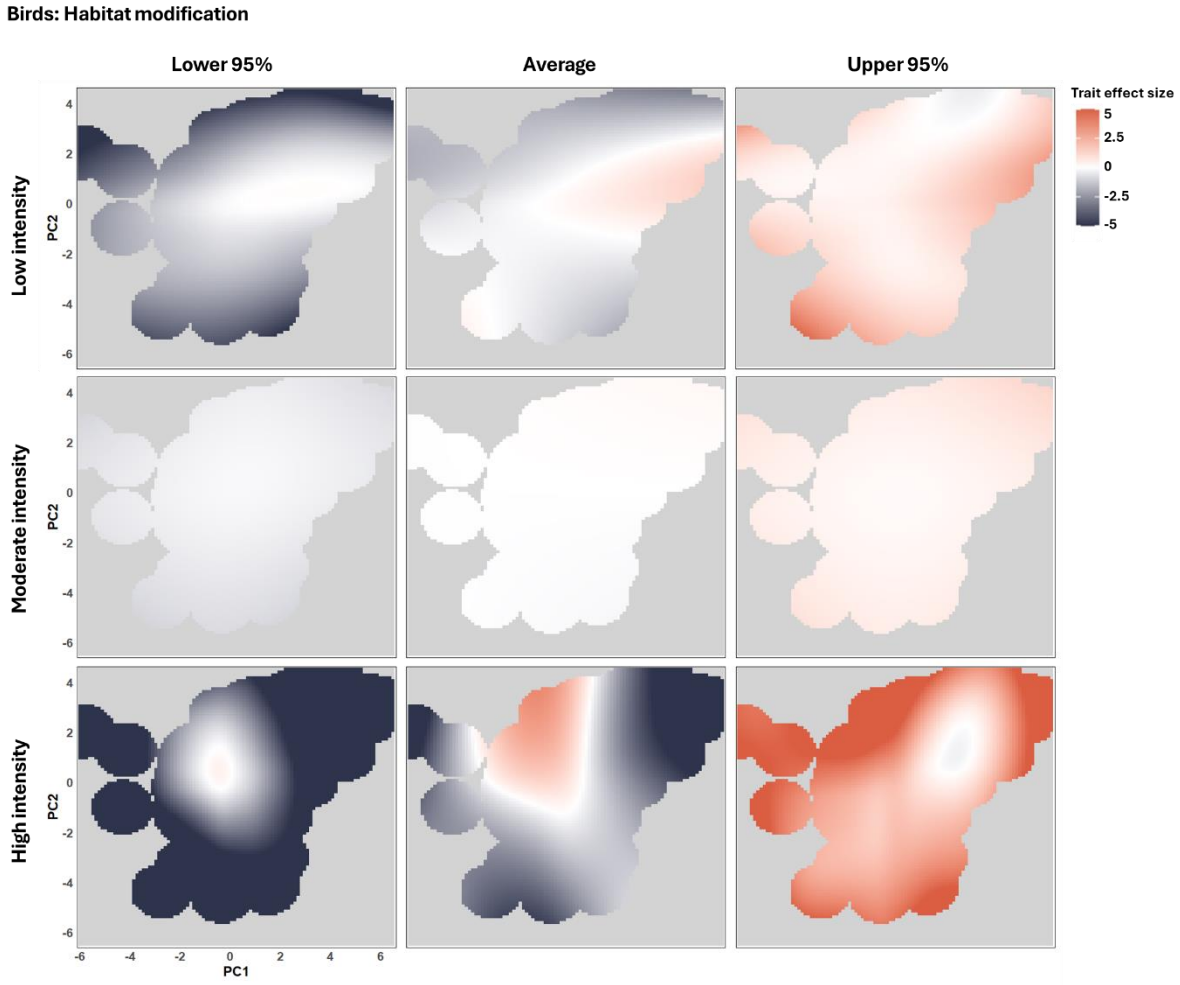

678 **Supplementary Figure 8: Upper and lower 95% confidence intervals for trait effect estimates for bird**
679 **responses to habitat modification across the bird life history trait space.** Predictions were obtained from
680 phylogenetically corrected GAMs, and pooled across imputations. Dark red represents positive effects of life
681 history traits on population response to threat (increased risk), whilst dark blue represents negative effects of
682 life history traits on response (decreased risk). White areas represent regions of low trait effects, where
683 response of populations is close to the average response attributable to intensity only. We do not extrapolate
684 responses for regions of the trait space that fall outside of the model spatial confidence intervals (grey areas,
685 based on distance from nearest data point). Columns represent the confidence intervals (left column: lower
686 95% interval; right: upper 95% interval) and average trait effect predictions (middle column) for each level of
687 threat intensity (top row: low intensity; middle row: moderate intensity; bottom row: high intensity).

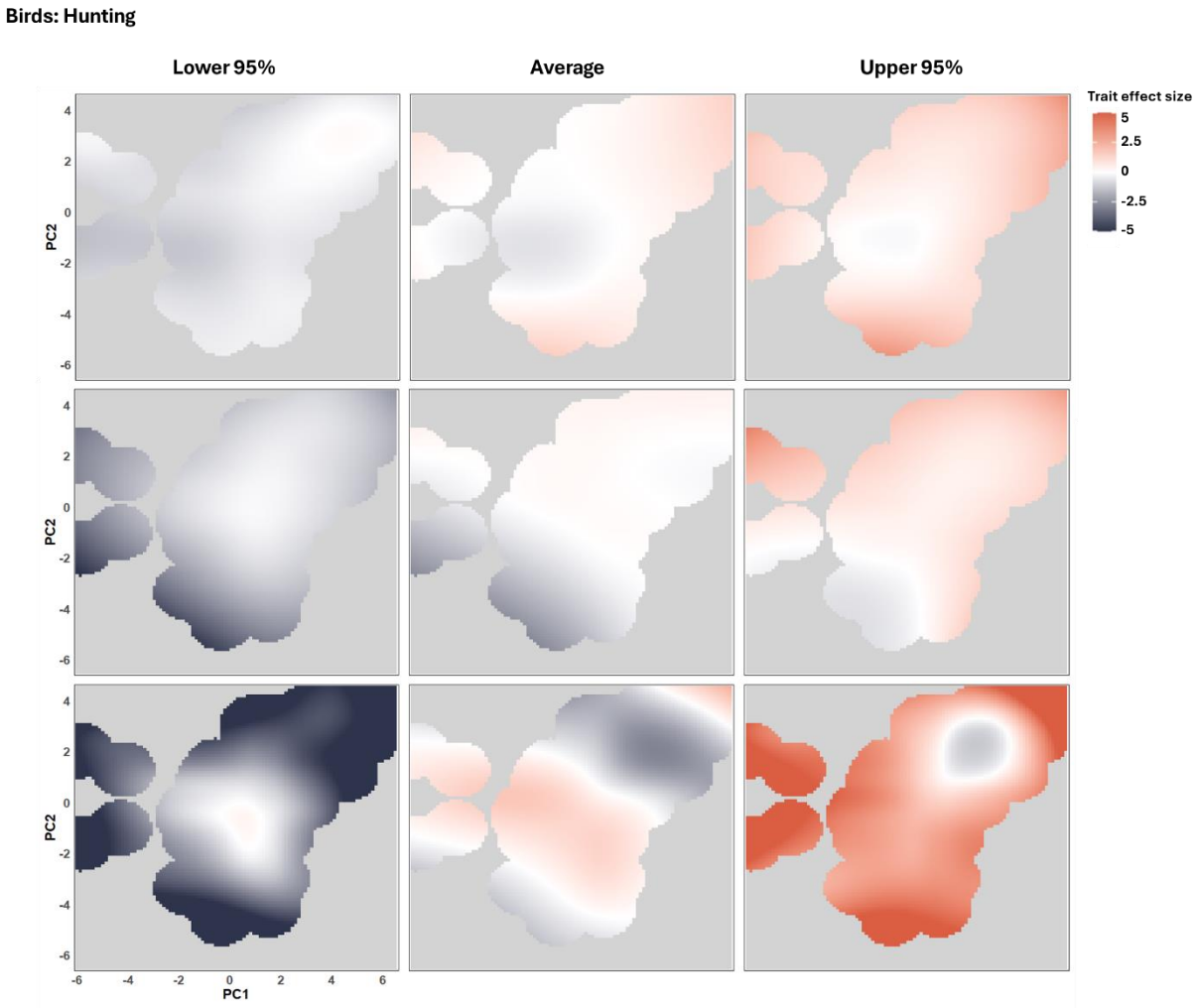

688 **Supplementary Figure 9: Upper and lower confidence intervals for trait effect estimates for bird**
689 **responses to hunting across the bird life history trait space.** Predictions were obtained from
690 phylogenetically corrected GAMs, and pooled across imputations. Dark red represents positive effects of life
691 history traits on population response to threat (increased risk), whilst dark blue represents negative effects of
692 life history traits on response (decreased risk). White areas represent regions of low trait effects, where
693 response of populations is close to the average response attributable to intensity only. We do not extrapolate
694 responses for regions of the trait space that fall outside of the model spatial confidence intervals (grey areas,
695 based on distance from nearest data point). Columns represent the confidence intervals (left column: lower
696 95% interval; right: upper 95% interval) and average trait effect predictions (middle column) for each level of
697 threat intensity (top row: low intensity; middle row: moderate intensity; bottom row: high intensity).

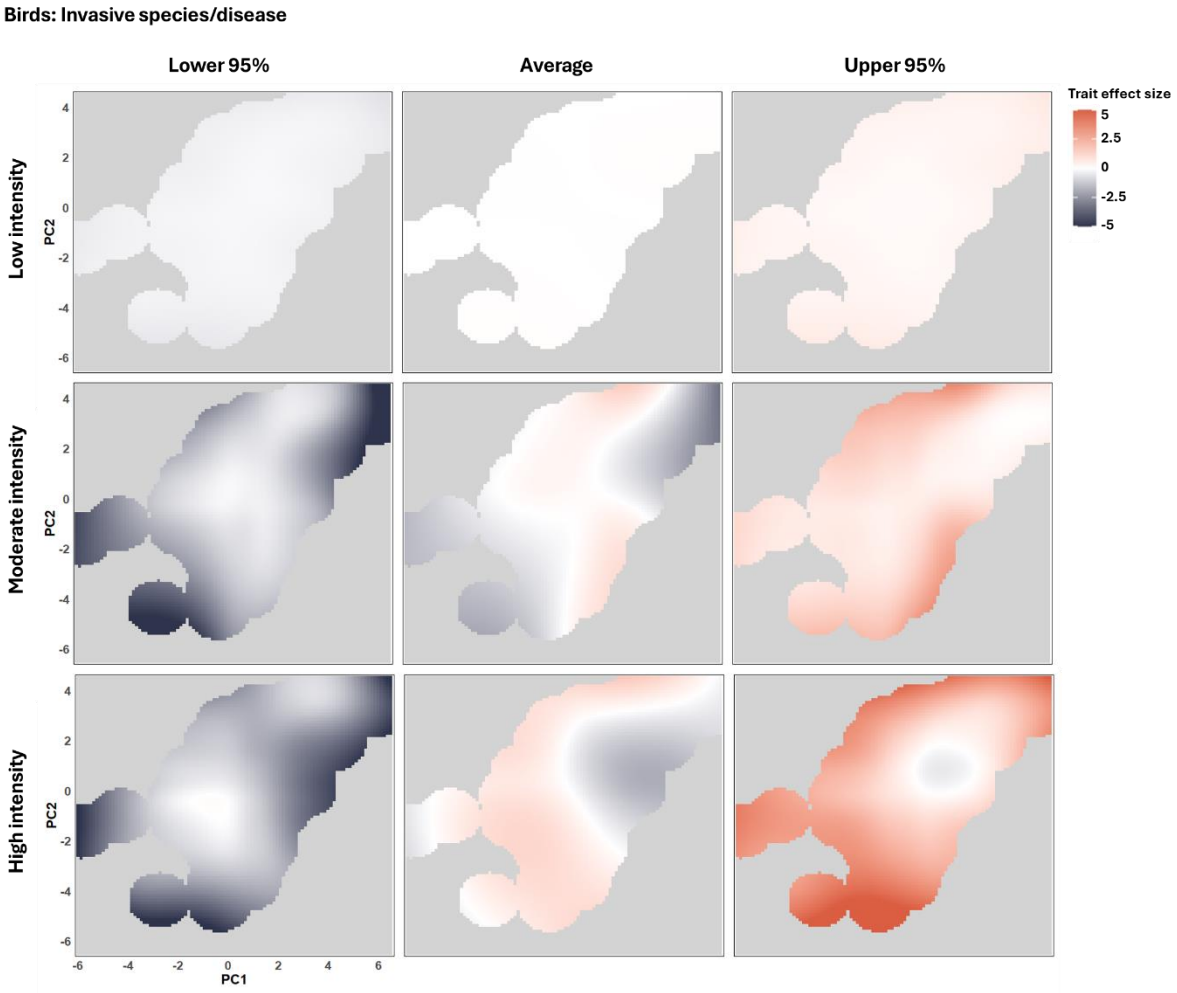

Supplementary Figure 10: Upper and lower confidence intervals for trait effect estimates for bird responses to invasive species/disease across the bird life history trait space. Predictions were obtained from phylogenetically corrected GAMs, and pooled across imputations. Dark red represents positive effects of life history traits on population response to threat (increased risk), whilst dark blue represents negative effects of life history traits on response (decreased risk). White areas represent regions of low trait effects, where response of populations is close to the average response attributable to intensity only. We do not extrapolate responses for regions of the trait space that fall outside of the model spatial confidence intervals (grey areas, based on distance from nearest data point). Columns represent the confidence intervals (left column: lower 95% interval; right: upper 95% interval) and average trait effect predictions (middle column) for each level of threat intensity (top row: low intensity; middle row: moderate intensity; bottom row: high intensity).

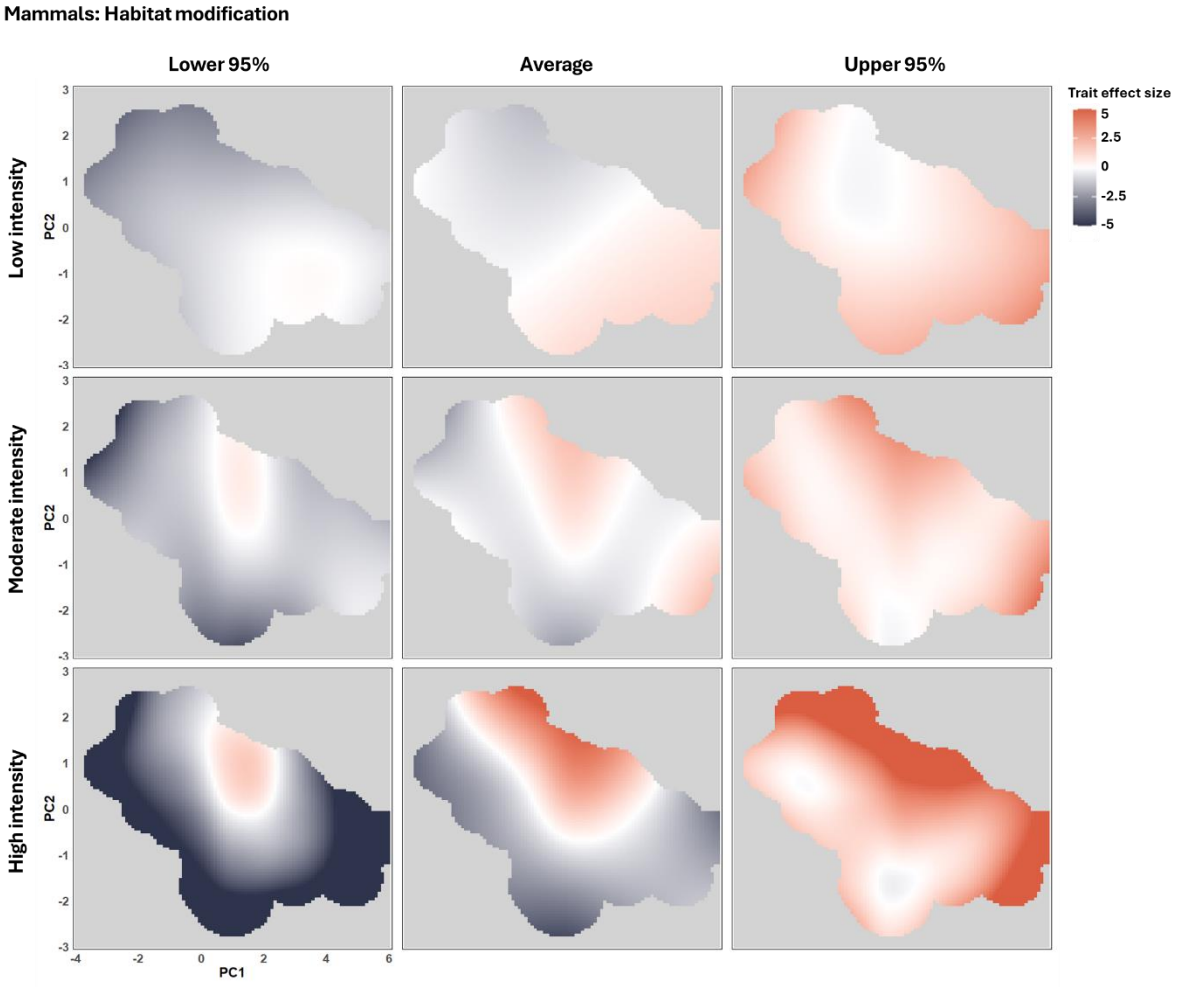

Supplementary Figure 11: Upper and lower confidence intervals for trait effect estimates for mammal responses to habitat modification across the mammal life history trait space. Predictions were obtained from phylogenetically corrected GAMs, and pooled across imputations. Dark red represents positive effects of life history traits on population response to threat (increased risk), whilst dark blue represents negative effects of life history traits on response (decreased risk). White areas represent regions of low trait effects, where response of populations is close to the average response attributable to intensity only. We do not extrapolate responses for regions of the trait space that fall outside of the model spatial confidence intervals (grey areas, based on distance from nearest data point). Columns represent the confidence intervals (left column: lower 95% interval; right: upper 95% interval) and average trait effect predictions (middle column) for each level of threat intensity (top row: low intensity; middle row: moderate intensity; bottom row: high intensity).

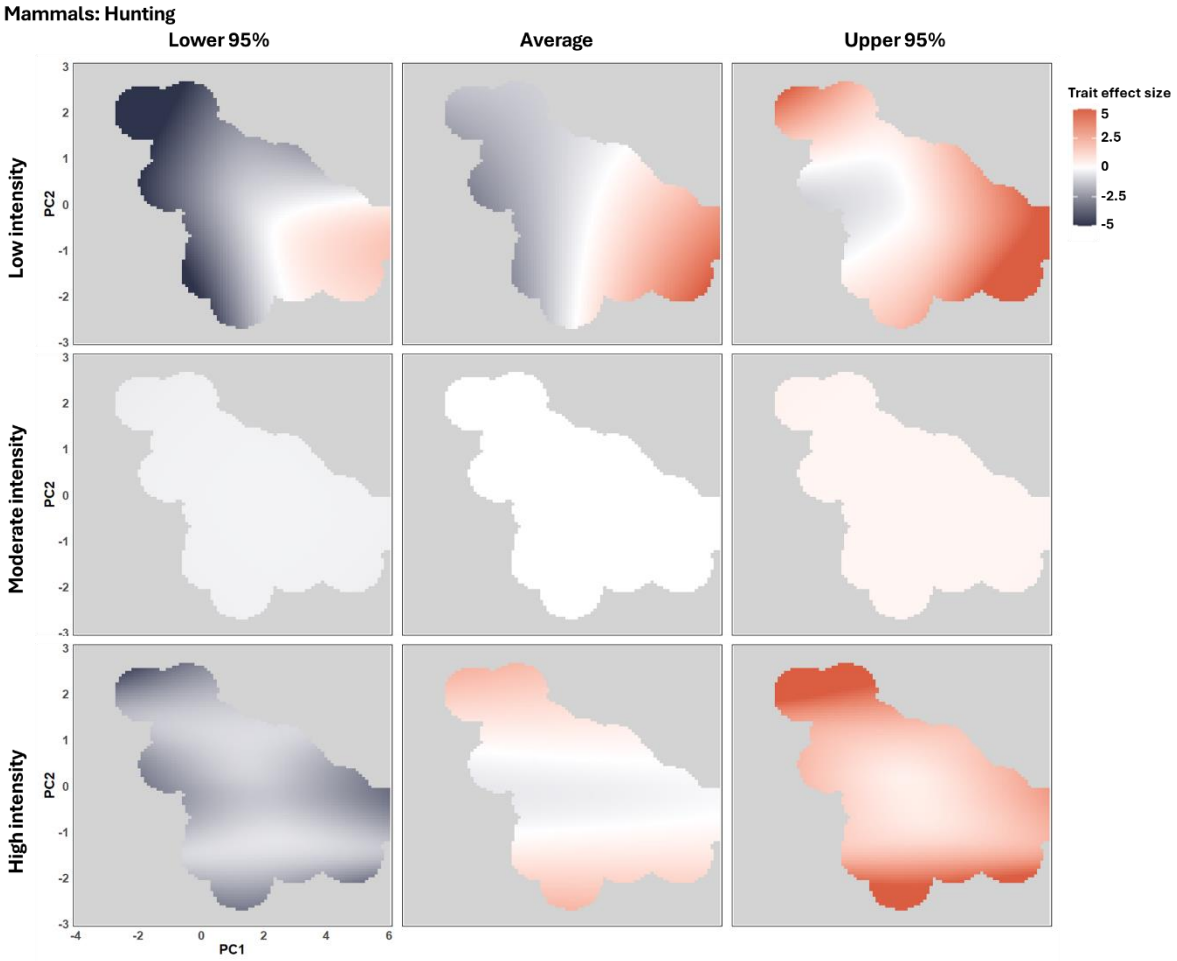

720 **Supplementary Figure 12: Upper and lower confidence intervals for trait effect estimates for mammal**
721 **responses to hunting across the mammal life history trait space.** Predictions were obtained from
722 phylogenetically corrected GAMs, and pooled across imputations. Dark red represents positive effects of life
723 history traits on population response to threat (increased risk), whilst dark blue represents negative effects of
724 life history traits on response (decreased risk). White areas represent regions of low trait effects, where
725 response of populations is close to the average response attributable to intensity only. We do not extrapolate
726 responses for regions of the trait space that fall outside of the model spatial confidence intervals (grey areas,
727 based on distance from nearest data point). Columns represent the confidence intervals (left column: lower
728 95% interval; right: upper 95% interval) and average trait effect predictions (middle column) for each level of
729 threat intensity (top row: low intensity; middle row: moderate intensity; bottom row: high intensity.

Supplementary references

1. Gower, J.C. and Dijksterhuis, G.B. (2004) Procrustes Problems. OUP Oxford
2. Van Ginkel, J.R. and Kroonenberg, P.M. (2014) 'Using Generalized Procrustes Analysis for Multiple Imputation in Principal Component Analysis', Journal of Classification, 31(2), pp. 242–269. Available at: https://doi.org/10.1007/s00357-014-9154-y
3. Josse, J., Pagès, J. and Husson, F. (2011) 'Multiple imputation in principal component analysis', Advances in Data Analysis and Classification, 5(3), pp. 231–246. Available at: https://doi.org/10.1007/s11634-011-0086-7
4. Van Ginkel, J.R. (2023) 'Handling Missing Data in Principal Component Analysis Using Multiple Imputation', in L.A. van der Ark, W.H.M. Emons, and R.R. Meijer (eds) Essays on Contemporary Psychometrics. Cham: Springer International Publishing, pp. 141–161. Available at: https://doi.org/10.1007/978-3-031-10370-4_8
5. Carmona, C.P. et al. (2021) 'Erosion of global functional diversity across the tree of life', Science Advances, 7(13), p. eabf2675. Available at: https://doi.org/10.1126/sciadv.abf2675
6. Gaillard, J.-M. et al. (1989) 'An Analysis of Demographic Tactics in Birds and Mammals', Oikos, 56(1), pp. 59–76. Available at: https://doi.org/10.2307/3566088
7. Stearns, S.C. (1977) 'The Evolution of Life History Traits: A Critique of the Theory and a Review of the Data', Annual Review of Ecology and Systematics, 8, pp. 145–171
8. IUCN. 2025. The IUCN Red List of Threatened Species. Version 2025-2. https://www.iucnredlist.org. Accessed March 2025.
9. Kleijn, D. *et al.* (2008) 'On the relationship between farmland biodiversity and land-use intensity in Europe', *Proceedings of the Royal Society B: Biological Sciences*, 276(1658), pp. 903–909. Available at: https://doi.org/10.1098/rspb.2008.1509
10. Nevoux, M. *et al.* (2013) 'The short- and long-term fitness consequences of natal dispersal in a wild bird population', *Ecology Letters*, 16(4), pp. 438–445. Available at: https://doi.org/10.1111/ele.12060
11. Germain, M. *et al.* (2017) 'Natal dispersers pay a lifetime cost to increased reproductive effort in a wild bird population', *Proceedings of the Royal Society B: Biological Sciences*, 284(1851), p. 20162445. Available at: https://doi.org/10.1098/rspb.2016.2445
12. Reed, D.H. (2004) 'Extinction risk in fragmented habitats', *Animal Conservation forum*, 7(2), pp. 181–191. Available at: https://doi.org/10.1017/S1367943004001313

13. Myhrvold, N.P. et al. (2015) ‘An amniote life-history database to perform comparative analyses with birds, mammals, and reptiles’, Ecology, 96(11), pp. 3109–3109. Available at: https://doi.org/10.1890/15-0846R.1.
14. Tierney, N. et al. (2023) ‘visdat: Preliminary Visualisation of Data’. Available at: https://cran.r-project.org/web/packages/visdat/index.html (Accessed: 14 April 2026).
15. Blomberg, S.P. and Todorov, O.S. (2025) ‘The fallacy of single imputation for trait databases: Use multiple imputation instead’, *Methods in Ecology and Evolution*, 16(4), pp. 658–667. Available at: https://doi.org/10.1111/2041-210X.14494.
16. Buuren, S. van and Groothuis-Oudshoorn, K. (2011) ‘mice: Multivariate Imputation by Chained Equations in R’, *Journal of Statistical Software*, 45, pp. 1–67. Available at: https://doi.org/10.18637/jss.v045.i03